IMPROVEMENT OF THERMO-SWITCH PROPERTIES IN POLYOLEFIN/CARBON BLACK COMPOSITES THROUGH THE ADDITION OF WAX

by

BENISON MOTLOUNG (B.Sc. Hons.)

Submitted in accordance with the requirements of the degree

MASTER OF SCIENCE (M.Sc.)

Department of Chemistry

Faculty of Natural and Agricultural Sciences

at the

UNIVERSITY OF THE FREE STATE (QWAQWA CAMPUS)

SUPERVISOR: PROF A.S. LUYT

CO-SUPERVISOR: DR D. DUDIĆ

March 2016

DECLARATION

I, the undersigned, hereby declare that the research in this thesis is my own original work, which has not partly or fully been previously submitted to any other university in order to obtain a degree. Furthermore, I cede copyright of the dissertation in favour of the University of the Free State.

_____

Motloung B. (Mr)

DEDICATION

This work is dedicated to my beloved family, Reuben Johannes Pienaar Motloung (father), Maditaba Letta Mofokeng (mother), Palesa Camellia Motloung (sister) and Thandolwethu Nkosinathi Mkhonza (nephew).

ABSTRACT

Conductive polymer composites (CPCs) based on LDPE, HDPE and iPP filled with carbon black (CB) and Zn micro-particles and blended with medium-soft wax were studied. The aim of this study was to investigate the effect of CB content, the presence of wax, γ-irradiation, and Zn metal powder as second filler on the thermal and mechanical properties, and thermo-electrical behaviour, of the composites. CB was used as the main filler to impart electrical conductivity to the composites. CB was generally not homogeneously dispersed in all the composites, while Zn was randomly dispersed with clear areas that were void of Zn, and agglomeration of Zn particles in other areas. It also seemed as if the dispersions did not depend on the type of polymer or the presence of wax, and as if there were a weaker interaction between CB and Zn than between CB particles. The crystallinities of the polymers generally decreased with an increase in CB loading, while the presence of Zn and/or wax gave rise to higher crystallinities. The presence of wax, however, had little influence on the melting and crystallization temperatures of the polymers. Irradiation reduced the crystallinities of the polymers in all the samples, as expected because of radiation-induced crosslinking. The storage modulus values of all the composites were higher than those of neat LDPE, although the presence of wax reduced these values, and the intensities of the α-transition depended on the type and amount of filler and on the presence of wax. All the composites show significantly lower resistivity than the neat polymers, and the resistivity decreased with increasing filler content. The 22 vol.% CB containing composites showed lower resistivities than the 12 vol.% CB + 10 vol.% Zn containing composites. The presence of wax caused a slight decrease in resistivity, while the irradiated samples generally showed higher resistivity values than the non-irradiated samples. The switching temperature shifted to higher values with increasing CB content, while it remained the same when part of the CB was replaced with Zn. Wax did not significantly influence the PTC intensity in the low CB content composites, but it caused a slight increase in PTC intensity in the Zn-containing samples. The irradiated samples generally showed an increased PTC intensity, but a reduced NTC intensity. All the samples showed a drop in resistivity after thermal ageing and good electrical stability during thermal cycling. The HDPE and iPP composites showed a fairly stable resistivity behaviour in the temperature range of investigation. Both the presence of filler and wax reduced the impact strengths of the composites.

LIST OF ABBREVIATIONS AND SYMBOLS

12CB	12 vol.% carbon black particles
12CB/10Zn	12 vol.% carbon black particles plus 10 vol.% zinc particles
22CB	22 vol.% carbon black particles
C15	Chain containing 15 carbon atoms in its backbone
C78	Chain containing 78 carbon atoms in its backbone
CB	Carbon black
CF	Carbon fibre
CNP	Carbon nanoparticle
CNT	Carbon nanotube
CPC	Conductive polymer composite
DBP	Dibenzoyl peroxide
DCP	Dicumyl peroxide
DMA	Dynamic mechanical analysis
DSC	Differential scanning calorimetry
DWCNT	Double-walled carbon nanotube
E	Electric field
E'	Storage modulus
E"	Loss modulus
EB	Electron beam
EG	Exfoliated graphite
EPDM	Ethylene propylene diene terpolymer (M-class)
EVA	Ethylene-vinyl acetate
GO	Graphene oxide
HDPE	High-density polyethylene
ΔH_m	Observed melting enthalpy
ΔH_m^n	Normalised melting enthalpy
ΔH_m^0	Specific melting enthalpy
I	Electric current
iPP	Isotactic polypropylene
LDPE	Low-density polyethylene
LLDPE	Linear low-density polyethylene
LMWPE	Low-molecular-weight polyethylene

MFI	Melt flow index
MWCNT	Multi-walled carbon nanotube
NTCR	Negative temperature coefficient of resistivity
PCM	Phase change material
PE	Polyethylene
PMMA	Poly(methyl methacrylate)
POM	Polarizing optical microscopy
PP	Polypropylene
PS	Polystyrene
PTCR	Positive temperature coefficient of resistivity
R	Resistivity
R_0	Specific resistivity
R_{70}	Resistivity at 70 °C
R_a	Resistivity after thermal ageing
rpm	Revolutions per minute
R_{rt}	Resistivity at room temperature
SEM	Scanning electron microscopy
SEM-EDS	Scanning electron microscopy-energy dispersive X-ray spectroscopy
T	Temperature
tan δ	Damping coefficient/loss factor
T_c	Crystallization peak temperature
T_g	Glass transition temperature
T_m	Melting peak temperature
UHMWPE	Ultra-high-molecular-weight polyethylene
V	Applied voltage
X_c	Degree of crystallinity

TABLE OF CONTENTS

LIST OF TABLES

LIST OF FIGURES

CHAPTER ONE

INTRODUCTION AND LITERATURE REVIEW

1.1 Introduction

Polymers, with special reference to plastics, are one of the most commercial and widespread materials in our life [1-3]. In their pure state, due to high electrical resistivity, with the exception of intrinsically conductive polymers, most of them are typical electrical insulators. However, doping them with various conductive fillers imparts conductive properties to polymers, resulting in the formation of conductive polymer composites (CPCs) [4]. These materials generally comprise a polymeric matrix into which a particulate filler is incorporated. Common conductive fillers include carbon black (CB), graphite and carbon fibre (CF), although other fillers such as carbon nanotubes (CNTs), graphene, metallic powders, flakes and fibres, as well as metallic oxides and hydrides have also been used [5,6]. CPCs are multifunctional materials, and can thus be routinely employed in various commercial applications due to their desirable properties such as good electrical conductivity, light weight, corrosion resistance and enhanced mechanical properties. Examples of applications for which CPCs can be employed include heating, shielding materials, actuators, self-heating plastics, electromagnetic radiation absorbing materials, battery and fuel cell electrodes, as well as anti-static, corrosion-resistant and positive temperature coefficient (PTC) materials [7,8].

Electrical resistivity (ρ), also known as specific electrical resistance, is an inherent property which indicates how strongly a given material opposes the flow of electric current. Its reciprocal, electrical conductivity (σ), also referred to as specific conductance, measures a material's capacity to conduct current. A low resistivity indicates a material that readily allows the movement of electric charge, and high resistivity is characteristic of a material that impedes the flow of charge. These materials can be termed electrical conductors and insulators, respectively.

The major applications for electrically conductive polymers and CPCs are governed by the magnitude of their volume resistivity. For insulation purposes, resistivity values above $10^{14}\ \Omega$ cm are required, while for anti-static applications, the range is 10^{9}-$10^{14}\ \Omega$ cm. For electrostatic

dissipation applications the range is 10^5-10^9 Ω cm, and for semi-conducting materials used in power cables to avoid partial discharge at the interface between the insulation and the conductor, the resistivity is around 10^3 Ω cm [9]. CBs are commonly preferred as fillers for conducting plastics and rubbers due to their low cost and density, relatively high electrical conductivity, and the specific structures that permit percolation at relatively low filler loadings. Metal powders are intrinsically more conductive than CB, but they are not as frequently used because of their tendency to oxidize and to form insulating layers on their surfaces.

Polymer composites need to undergo an insulator-conductor transition to be conductive. This occurs when electrically conductive filler is randomly dispersed in a non-conductive polymer matrix above a critical concentration [10,11]. At low filler contents the conducting particles are dispersed within polymeric matrix as isolated clusters, while above a critical concentration of the filler, the clusters begin to join and form paths of inter-connected filler particles, which results in a conductive network throughout the entire composite. This critical concentration is referred to as the percolation threshold, and at this transition the composite undergoes a several orders of magnitude increase in conductivity and dielectric properties [12]. It is crucial to obtain conducting composites with the lowest possible volume fraction of conducting particles so as to avoid high costs but still retain easy processability. Conductive filler increases the effective conductivity of the composites, and the most important volume fraction is the one slightly above the percolation threshold. When the filler loading is below the critical concentration, the composites are anti-electrostatic and can thus be employed for anti-static applications. However, above the threshold, the percolated composites are suitable for electrical switching.

Electrical switching can be attained by using a material whose resistivity increases sharply as a consequence of a certain circumstance, e.g., when the temperature or electric field rises beyond a threshold value. The switching provides protection for electronic devices from damage caused by exceeding the threshold. Semi-crystalline polymers filled with electrically conductive particles are usually employed for electrical switching. Conductive fillers such as CB, graphite, coke, CFs and titanium diboride (TiB_2) have been utilized for electrical switching. However, due to its low cost and particulate nature, CB is the most preferred filler. Effective “switching” materials usually contain filler contents slightly above the upper limit of the percolation region [13-16]. There are two phenomena involved in electrical switching:

positive temperature coefficient of resistivity (PTCR) and negative temperature coefficient of resistivity (NTCR). The former takes place just before the melting point of the matrix while the latter occurs after melting of the polymer crystals.

Near the polymer melting region, carbon-filled composites exhibit a drastic resistivity increase with an increase in temperature [17-19]. The matrix undergoes a rapid expansion in the vicinity of melting, and since the thermal expansion coefficient of the polymer matrix is larger than that of the filler, voids are formed between filler particles and aggregates, that break the conductive pathways and hinder conduction. This phenomenon is known as the positive temperature coefficient (PTC) effect, and the abrupt rise in resistivity provides switching [20]. The negative temperature coefficient (NTC) effect occurs immediately after the switching. As the polymer melts, conductive paths form again and distribute as agglomerates in the melt, rendering the composites conductive again. This is a consequence of the relaxation of the polymer structure due to the low viscosity of the matrix at high temperatures, which significantly increases the mobility of the CB particles in the composites [21,22]. The PTC phenomenon is a disadvantage in cable engineering, but it can be successfully used in several other industrial applications, such as self-regulating electric heaters, current limiters, overcurrent protectors and various sensors involving temperature fluctuations [23].

Just like any other system, thermo-switch materials have their flaws. Examples include the instability of the resistivity behaviour with temperature due to the presence of the NTC effect, which causes the PTC effect to lose its significance. Furthermore, where high conductivity is a requirement, satisfactory switching behaviour is seldom achieved. Generally, low-conductivity materials exhibit significant switching behaviour, while high-conductivity composites show poor switching behavior [13-16]. Since the NTC effect is a disadvantage in switching applications, practical methods to eliminate it include crosslinking, either chemically with peroxides or by irradiation with electron beam (EB) or γ-rays [14]. Adding rubber as a ‘mechanical stabilizer’ to CB/wax mixtures [24] and using mixtures of two kinds of CB with polyethylene (PE) [13] have also been employed. CB particles apparently become attached to or entrapped in the crosslinked network, and crosslinking increases the viscosity of the matrix resulting in a marked reduction of movement of intermolecular segments, which fixates the structure and decreases the carbon particle freedom of movement, preventing them from re-agglomerating above the polymer melting temperatures [6]. When ultra-high

molecular weight polyethylene (UHMWPE) was used as one of the blend components [19,25-27], the reproducibility of the resistivity behaviour was satisfactory, since UHMWPE minimizes the migration of the conductive particles due to its high viscosity even at elevated temperatures.

1.2 Literature review

1.2.1 Polymer/wax blends

Blending of paraffin wax with polyolefins is well documented in literature [28-42]. Various processing techniques such as melt-mixing, melt-extrusion and mechanical methods were used to prepare the blends. Melt-mixing proved to be more appealing to most researchers, probably due to its quick, simple and cost-effective mode of operation. Different grades of paraffin wax with different melting temperatures were utilized, including medium-soft, hard and oxidized paraffin wax. These grades of paraffin wax gave rise to different physical properties, depending on the type of polymer used. Various microscopic techniques were used to determine the morphology of the blends, and different grades of paraffin wax gave rise to different morphologies. The authors reported mainly on phase-separation, continuity, and interfacial interaction of the blend components.

In one study, polypropylene (PP) was investigated as a potential matrix for the creation of shape-stabilized phase change materials (PCMs) [37]. Separate crystal fractions were observed for PP and wax and there was also no indication of co-crystallization on micro level, suggesting complete immiscibility between the two components. Low-density polyethylene (LDPE) exhibited different morphologies when blended with hard and soft paraffin wax [32]. The former blend showed a fairly homogeneous surface with only a slight indication of wax separation, while pronounced phase separation was clearly observed in the latter case. Since the crystalline structure is the same for both types of waxes, the different behaviour of these waxes was attributed to their different molecular weights. Apparently soft wax, due to its lower molecular weight and resulting lower viscosity, was able to separate from the blends much easier than hard wax with its higher molecular weight. In high-density polyethylene (HDPE)/wax blends [40-41], paraffin wax was found to be compatible with HDPE since the former is a homologous compound of the latter, i.e. they have similar chemical structures. The

authors observed that paraffin, which was employed as a PCM, was fairly well dispersed in the three-dimensional net structure formed by HDPE, which acted as a supporting material.

The thermal properties of polymer/wax blends were determined using differential scanning calorimetry (DSC). The authors reported mainly on the effect of wax on the melting temperatures, multiplicity of endothermic peaks as well as the melting enthalpy values of the polymers. Blending of wax with different polymers produced different behaviour, depending on the grade of wax used or the type of the matrix employed. It was generally observed that increasing the wax content induced a reduction in the melting temperatures [30,32,35,39-40,42] and an increase in the melting enthalpies of the blends [28-29,31-32,36,39,42]. However, an increase in the wax content of the blends did not influence the melting temperatures in certain studies [29,33]. Paraffin wax was also found to be mostly miscible with the polyolefins in the crystalline phase at low wax contents, forming a single endothermic peak in the blends. However, at higher wax contents, multiple endothermic peaks were observed, which corresponded to the melting peaks of pure components, thus suggesting partial or no miscibility. The thermal behaviour of low and high molecular weight paraffin waxes used for designing PCMs was investigated in one study [43]. In its unblended state, soft wax exhibited two well-resolved endothermic peaks. The low-temperature endothermic peak was attributed to a solid-solid transition, while the higher temperature endothermic peak was due to a solid-liquid transition.

Comparison of LDPE, LLDPE and HDPE as matrices for PCMs based on a soft Fischer–Tropsch paraffin wax was investigated in another study [30]. Two clearly defined endothermic events were observed for all the blends – the first event corresponded to the transitions within the wax structure while the second event was associated with the melting of the polymer crystallites. The melting peak temperature of LDPE in the blend was significantly lower than that of the pure polymer, and the temperature further decreased with increasing wax content. This behaviour was probably the result of the molten wax which had a softening effect on the matrix. This effect was more pronounced in HDPE, because paraffin wax had the lowest miscibility with HDPE, and it therefore had the strongest influence on its melting temperature.

PP was also blended with paraffin wax [37-38]. In the one study, a single endothermic peak was observed at very low wax contents, since PP and wax can in principle not be miscible due

to different crystallization behaviours, this was ascribed to macroscopic homogeneity at this concentration. At higher concentrations of wax, two other significant peaks were observed, implying that no macroscopic homogeneity was observed in the solid state. An increase in wax content slowly led to a decrease in melting temperatures and an increase in the specific enthalpy of melting. Complete immiscibility of soft and hard wax with PP was observed in the other study. The melting point of the PP component in the blends decreased with an increase in wax content, which indicated a softening effect on the PP by both waxes. The specific melting enthalpy related to the wax content increased with an increase in wax content, whereas that related to the PP content decreased.

Dynamic mechanical analysis (DMA) was used to investigate the thermo-mechanical properties of paraffin wax blends. The effect of wax on the storage modulus, loss tangent and to a lesser extent loss modulus of the polymer was investigated. Different relaxations, i.e. α, β and γ, were observed, and wax was found to generally reinforce the matrices below their melting temperatures, softening them in their molten states. For example, this behavior was observed when LDPE was blended with hard and soft paraffin waxes [32]. The latter reinforced the PE matrix below its melting temperature by acting as a highly crystalline filler that immobilized the polymer chains at the crystal surface. However, this matrix reinforcement, which also yielded high modulus values, did not seem to depend on wax concentration in the studied concentration range. For loss tangent in injection-molded HDPE/wax blends [35], neat HDPE displayed a single peak and in the case of the blends, two peaks were observed. The first one corresponded to an α-relaxation (T_g) of PE, while the second one represented the T_g of paraffin wax. This was attributed to the immiscibility between the components of the blend. For the storage modulus, two kinds of behaviour were identified in the vicinity of the melting temperature of wax. In its solid state, paraffin wax reinforced the PE matrix by immobilizing the polymer chains, leading to a higher modulus of the polymer. However, above the wax melting, the decrease of the modulus was more pronounced, especially in the blends containing higher wax content.

PP was also blended with soft and hard paraffin waxes [37]. In the case of the former, increasing the wax content induced a corresponding drop in the storage modulus, which was attributed to the plasticizing effect of the PP matrix by the wax component. This was a consequence of the changes in mechanical properties due to different structures and especially molar masses of the components. There was only a slight change in elastic modulus at lower

temperatures, and the observed relaxation peak was attributed to a solid-solid transition in the wax. The first relaxation peak of PP overlapped the wax melting peak, while the second relaxation peak of PP, which occurred below its melting, was shifted to lower temperatures in the blends. The melting temperature of the material generally decreased with an increase in wax content, and the effect was more pronounced in the blends with high wax contents.

The effect of crosslinking on the properties of blends of polyolefins with wax was investigated in a few studies. Dicumyl peroxide (DCP) [29, 34] and dibenzoyl peroxide (DBP) [31] were used as crosslinking agents. Increasing the content of the crosslinking agent generally yielded a corresponding increase in the gel content, and thus the crosslink density of the blends. It was observed that the gel content generally decreased with an increase in wax content, possibly due to the low molecular weight of wax. It was also noted that because of wax' short chains, the peroxides were not effective in small concentrations to sufficiently crosslink the wax chains in the blends to form an insoluble network. However, at high concentrations, the crosslinking agents seemed to be more effective, even at high wax contents, suggesting that wax also contributed to the final gel content, hence a much higher gel content was measured. At low peroxide concentrations, only the PE phase was crosslinked, because wax needed a much higher concentration of peroxide for crosslinking. Crosslinking was found to generally reduce the crystallinity of the blends, causing the crystallization temperature to decrease with an increase in peroxide concentration.

1.2.2 Conductive polymer composites

A variety of electrically conductive fillers with different dimensions were used to prepare CPCs, amongst which were CB, CNT, CF and graphite. Different processing techniques such as melt-mixing, solution-mixing, mechanical-mixing and emulsion copolymerization were used to prepare the composites. A number of studies investigated the morphology of CPCs [6,44-46]. In PP/CB composites [46], carbon particles were interconnected in a network, suggesting that the system had already percolated. In HDPE/CB composites [6], due to the action of radiation, a sol-gel structure was observed and the CB particles were dispersed in and bound to the crosslinked networks (gel), which significantly limited the movement of these particles. In paraffin wax/graphite composites, the nano-platelets were either embedded in the paraffin matrix or lying on the surface. It was reported that the particles in paraffin nano-composites maintained their platelet-like shape due to the low viscosity of the polymer

matrix [44]. However, in another study [45], it was observed that the dispersion of the graphite particles in the paraffin wax was uniform. The nano-platelets were fairly well-dispersed in the paraffin, and were even slightly covered by the paraffin. In iPP/carbon nano-particle (CNP) composites [47], CNPs were finely dispersed in the iPP matrix at low filler contents. However, at higher loadings, there was a tendency to form agglomerates.

Combining different conductive fillers can significantly improve the electrical conductivity of CPCs. Graphite, CB, CF, multi-walled carbon nanotubes (MWCNTs), double-walled carbon nanotubes (DWCNTs), bismuth telluride (Bi_2Te_3) and silver flakes have been used to create hybrid fillers. The hybrid composites were prepared through methods such as mechanical-mixing, solution-mixing and melt-mixing. The composites generally exhibited good electrical conductivity and better dispersion in the matrices. In one study [49], UHMWPE granules were coated with a CNT/Bi_2Te_3 hybrid filler, and a segregated network in which the conducting CNT/Bi_2Te_3 layers were predominantly located at the interfaces between UHMWPE granules was formed throughout the composite. The addition of graphite oxide (GO) sheets to MWCNTs greatly reduced the size of their aggregates, and improved their dispersion [50]. Apparently the MWNTs linked up with the GO sheets, which promoted the formation of a conductive network at a much lower filler content compared to pristine MWNTs, causing the hybrid filler to disperse uniformly in the PP matrix. In silver-filled hybrid composites [51], the dispersion of DWCNTs in the hybrid composite led to the formation of agglomerates of very long CNT bundles, while MWCNTs were more individualized and well-dispersed between the silver flakes. This was attributed to the very high surface areas of the DWCNTs. A synergistic effect was found in MWCNTs/CB hybrid filler composites [52], where CB addition improved the MWCNT dispersion and also reduced the size of big primary nanotube agglomerates. In PP/CF/CB composites [53], both the CF and CB particles were uniformly distributed in the PP matrix and the hybrid structure of the filler was successfully formed.

The thermal properties of paraffin wax/exfoliated graphite (EG) composites were investigated [44]. It was observed that the melting and crystallization temperatures were not significantly affected by the addition of the nano-platelets. The melting and crystallization enthalpies for the paraffin nano-composites were similar to that of the neat paraffin at low filler concentrations. However, at high loading levels, the composite's ability to absorb and release heat was degraded because of the increasing replacement of paraffin wax with filler particles.

It was also noted that the incorporation of graphite particles into the paraffin wax did not reduce its phase-change efficiency. Rather, an increase in filler content led to a slight improvement in the wax' heat absorbing and releasing capacity. Similar results were obtained in another study [45], where it was reported that the thermal characteristics of the composite PCM were very close to those of the pure paraffin. This was because there was no chemical reaction between the paraffin and the EG in the preparation of the composite PCM. In PP/graphene [54] composites, the values of the melting temperature and the degree of crystallinity did not change significantly with filler addition. However, a significant increase in the crystallization temperature indicated that the graphene nano-sheets were acting as nucleating agents in the nano-composites.

The effect of annealing on the thermal properties of LDPE/CB composites were investigated in one study [55]. It was observed that the peak temperatures of phase transitions of the polymer matrix were higher for the annealed samples, and the crystallization of the polymer matrix tended to be more perfect with an increase in annealing temperature. Due to the reduced volume fraction of the amorphous region, the dispersed CB particles were more compressed, and the filler content per unit volume increased, resulting in lower resistivity at room temperature which made the PTC intensity increase. In an investigation of the thermal properties of recycled PP/CB composites, it was found that the enthalpy of fusion was higher for the recycled PP compared to that of the pristine PP [46], and the difference was attributed to a decrease in the molecular weight due to degradation. In iPP/CNP nano-composites [47], there was a clear shift in melting temperature to higher values, which was attributed to the crystallization effect of the CNPs. Apparently CNPs can act as a nucleating agents, increasing the rate of crystal formation, but significantly reducing the size of the formed crystallites.

CNPs imparted a toughening effect on the polymer in iPP/CNP nano-composites [47], and the storage modulus increased with an increase in the CNP content at low temperatures. However, this increase was less obvious at higher temperatures, since the mobility of the iPP macromolecules was very high above its T_g. At low CNP concentrations, the T_gs of the nano-composites were almost the same as those of the neat polymer. Usually, the T_g of a polymer matrix tends to increase with the addition of nanoparticles, due to the interactions between the polymeric chains and the reduction of their mobility at the interface around the nanoparticles. In this case, weak changes in the glass transition temperature were observed, probably due to agglomeration of the CNPs at a higher filler content. An increase in the storage modulus with

increasing graphene nano-sheet content was observed in PP/graphene nano-composites [54], which was attributed to the reinforcing effect of the graphene. However, this effect was more significant above the T_g when the PP chain mobility was sufficiently high, and it was higher in the iPP materials prepared by *in situ* polymerization than in the solution-blended nano-composites [56]. The rigidity imparted by the graphene slightly modified the amorphous regions, and small differences were observed in the location and intensity of the β-transition, causing it to move slightly to higher temperatures. Due to changes in the mobility within the crystallites, the α-transition also shifted to higher temperatures, and its intensity in the nano-composites was lower than that in the neat iPP.

In investigations of the thermo-electrical properties of conductive polymer composites it was found that, in HDPE/CB composites, crosslinking slightly increased the resistivity of the materials, and increasing the radiation dose caused an increase in the PTC intensity and totally eliminated the NTC effect [6]. The influence of crystalline and aggregate structures on the PTC characteristics of conductive PE/CB composites was also investigated [55]. The resistivity behaviour of HDPE/CB, LDPE/CB, EVA/LDPE/CB and PMMA/CB were compared. All the composites exhibited both PTC and NTC effects, but the PTC intensity of the PMMA/CB system was very weak because of its amorphous nature. HDPE/CB showed the highest PTC intensity due to the larger expansion accompanying crystalline melting. In the LDPE/CB composites, the PTC intensity increased with an increase in annealing temperature while the NTC intensity decreased. This implied an improvement in the switching sensitivity. The PTC intensity initially increased with increasing annealing time, but levelled off at longer annealing times.

The electrical properties of hybrid composites were investigated in a few studies [48-50,53]. In one study [48], CF and graphite blend composites were compared. The PTC of the CPCs containing CF was markedly lower than that of the CPCs with graphite. Conductivity was also observed to be more strongly dependent on filler concentration in the CF-based CPCs than in the graphite-based materials. This was attributed to the relatively longer CF particles, which were more likely to form continuous conductive pathways in the polymer blend. The graphite/CF hybrid filler exhibited significantly higher conductivity than the neat graphite. Apparently the CF bridged the separated and unconnected graphite particles, thereby increasing the net conductivity of the composites. Similar results were obtained in another study [49], where the thermo-electric behaviour of segregated CPCs with hybrid fillers of

CNTs and Bi_2Te_3 was investigated. At a high CNT loading, the electrical conductivity of the hybrid composites increased, suggesting the Bi_2Te_3 particles had a positive impact on the formation of CNT networks. Improved electrical conductivity was also observed in PP/GO/MWNTs composites [50], indicating that hybrid fillers more easily formed effective and continuous conducting paths or networks in a PP matrix than pristine MWCNTs. Incorporation of CB into PP/CF composites also improved the conductivity with an increased loading of CF [53]. The significant improvements in the electrical conductivity of the composites were attributed to the formation of effective three-dimensional conductive pathways composed of CF and CB in the PP matrix.

The effect of crosslinking on the electrical properties of conducting composites was investigated in a few studies where EB [6,10] and γ-irradiation [57] were used. Since CB particles locate in the amorphous regions of semi-crystalline polymers, and because the crosslinking by irradiation also takes place preferentially in the amorphous regions [58], the freedom of movement of the CB particles may be reduced as a consequence of the shrinking of the amorphous phase induced by irradiation and the formation of crosslinks. In HDPE/CB composites [10], crosslinking was very effective in stabilizing the percolation network. The significant improvement in the conduction stability, even after electric field action, was ascribed to the restricted mobility of the polymer chains in the amorphous region where the CB particles were dispersed. In UHMWPE/CB composites [57], increasing the filler content led to a significant increase in surface conductivity at low irradiation doses. However, higher irradiation doses caused the breaking of the conductive carbon chains on the composite surface due to increased crosslink density, which led to a sharp decrease in conductivity.

1.2.3 Polymer blend composites

These composites are usually prepared *via* melt-mixing, while other processing techniques such as solution-mixing and mechanical-mixing have also been employed. Different morphologies were obtained owing to various kinds of fillers with different dimensions. In LDPE/paraffin/graphite blend composites [59], it was observed that paraffin and LDPE were mixed uniformly and formed a dense network into which the graphite particles were uniformly dispersed. EG [60] showed much better dispersion of the smaller graphite particles and a more well-defined thermally conductive network. In conducting CB/PP/EVA composites, the distribution of CB in the blend was in the form of distinct particles below the

percolation threshold. However, above this critical concentration, the filler was in the form of fibrils that formed aggregates. An obvious percolation network was formed by these aggregates, rather than the individual particles [61].

In a study where LDPE, LLDPE and HDPE were blended with paraffin wax and filled with copper (Cu) particles, the composites generally showed a two-phase morphology, which suggested immiscibility between the PE and the wax [62]. The copper particles were covered by a wax layer, which indicated that the Cu particles had a higher affinity for the wax. This preferable crystallization of the wax onto the Cu particles was attributed to the incompatibility of the wax and the PEs, as well as to the thermodynamically more preferred adsorption of the smaller wax molecules onto the rough Cu surfaces. Crosslinked HDPE particles were incorporated in HDPE/CB composites in another study [18], and a two-phase morphology was observed. The CB particles were dispersed in the HDPE phase, and the addition of crosslinked HDPE particles increased the effective CB concentration in the HDPE matrix and thus lowered the room-temperature resistivity of the composites. In another study [63], it was found that CF particles oriented randomly in the LMWPE/UHMWPE blends. At low filler content most of the fibres were detached, but at higher loadings most fibres were connected with each other, forming conducting paths. However, voids were also observed, which indicated incomplete adhesion between the PE and the CF particles.

In PP/polystyrene (PS)/CB blend composites [11], CB was found to preferentially localize in the PS phase due to the differences in chemical affinity between the polymers and the additive filler. A two-phase morphology was also observed in PP/UHMWPE/CB composites [19]. The CB particles were situated at the interface between the two polymers. After saturation, due to the high viscosity of UHMWPE, the CB particles were forced to further disperse in the continuous PP phase.

Investigation of the thermal properties of a new kind of shape-stabilized PCM with PTC effect showed two endothermic events [59]. The first was characterized by solid-solid as well as solid-liquid transitions in the paraffin, while the second event showed a small solid-liquid transition for LDPE due to its low content in the PCM. The switching temperatures were determined by the solid–solid, as well as the solid-liquid, phase transitions of the paraffin, which occurred at about 25 and 45 °C, respectively. The temperatures at which the PTC effects of the materials occurred were therefore related to the phase change temperatures of

paraffin in the PCM. Thermally conductive PCMs for energy storage based on LDPE, soft Fischer–Tropsch wax and graphite were also studied [60]. Two endothermic peaks for wax were observed for pure wax, but when blended with LDPE, even in the presence of graphite, there was a peak shoulder just after the main peak, which could have been the result of co-crystallization of the lower molecular weight fractions of the LDPE with the wax. Pure LDPE also exhibited two endothermic peaks, but only one peak was observed in the blends, which was attributed to the molten wax in some way inhibiting the crystallization of the LDPE. The presence, type and amount of graphite did not really influence the crystallization and melting behaviour of the wax and LDPE. In CB/PP/EVA blend composites [61] the addition of EVA and CB led to a decrease in the melting temperatures and enthalpies, indicating a decrease in the crystallinity of the PP.

For LDPE/wax/Cu, LLDPE/wax/Cu and HDPE/wax/Cu blend composites [62], it was reported that the presence of Cu micro-particles did not significantly affect the thermal behaviour of the PE/wax blends, even though the wax seemed to have a higher affinity for Cu and preferably crystallized on its surface. The introduction of CF also did not have a significant effect on the thermal properties of LMWPE/UHMWPE blends. The crystallinity and grain size were found to be independent of CF contents.

An investigation of the thermo-mechanical properties of LDPE/wax/graphite blend composites showed that the presence of wax reduced the storage modulus of LDPE below and above its glass transition [60]. This decrease was quite significant above the wax melting temperature. This was attributed to the softening effect of wax on the matrix. Increasing the graphite content increased the storage modulus, with this effect being more significant for EG. The blends with higher graphite contents had storage modulus values of the same order of magnitude as those of LDPE, indicating that the presence of graphite reinforced the composites and countered the softening effect of the wax. The T_g of LDPE broadened and shifted to higher temperatures because the wax crystals and graphite particles in the amorphous phase of the LDPE immobilized the polymer chains.

The thermo-electrical properties of PCMs and other blends were investigated in a few studies [18-19,59,63-64]. Generally the low molecular weight (i.e. low melting point) components determined the PTC temperature in the composites. The composites exhibited a double PTC effect at temperatures corresponding to the solid-solid and solid-liquid transitions of wax [59].

The wax composites showed a sharp decrease in resistivity above its melting temperature, while no NTC effect was observed when n-alkanes were used as blending components [64]. The graphite content, as well as the mass proportions of LDPE/paraffin had no influence on the temperatures at which the PTC and NTC phenomena occurred. Another study [61] found that the addition of EVA to CB/PP composites was essential in the formation of conductive paths. The incorporation of the crosslinked HDPE particles in HDPE/CB composites led to a decrease in room-temperature resistivity [18]. Apparently the crosslinked HDPE played the role of a filler which increased the CB volume fraction in the HDPE matrix. In PP/UHMWPE composites a sharp increase in the resistivity of the composites occurred in a similar temperature range as the melting of the UHMWPE and PP crystallites [19], which was termed the double PTC effect. The PTC effects observed around the melting temperatures of the semi-crystalline polymers were attributed to the volume expansion as a result of the melting of UHMWPE and PP crystallites, and the PTC intensities strongly depended on the CB content. Usually low CB content composites showed a higher room temperature resistivity and PTC intensity, while high CB content showed a lower room temperature resistivity and PTC intensity. A better PTC effect was observed for LMWPE and UHMWPE blends containing CF blends than for the comparable CB containing blends [63]. At the melting temperature of LMWPE, the thermal expansion of LMWPE was restricted by the solid UHMWPE, enabling the CF to maintain good electrical conductivity. However, an abrupt resistivity rise was observed at the onset of the melting of the UHMWPE, which resulted from the breaking of the conductive paths. The PTC effect was found to be dependent on the CF content.

Certain studies demonstrated the effect of radiation crosslinking on the resistivity behaviour of the blend composites [18,23]. EB and γ-irradiation were used to crosslink the blend composites. The degree of crosslinking generally increased with increasing irradiation dose, but the gel content of the EB-irradiated compounds was higher than that of the γ-ray irradiated composites. This was attributed to the dose rate effect. An increase in the gel content induced an increase in the room temperature resistivity and a decrease in NTC intensity. For example, in a HDPE/crosslinked HDPE/CB system [18], at low irradiation doses, increasing the γ-irradiation dose caused a slight decrease in the PTC intensity, and the composites exhibited an NTC effect above the melting temperature of the HDPE. In contrast, EB irradiation effectively eliminated the NTC effect at lower doses compared to the γ-irradiation. A small NTC effect was observed in uncrosslinked PE/EPDM/EVA/CB composites, while a sharp

NTC effect was observed in HDPE/CB systems [23]. This was attributed to the inclusion of elastomers and different CB characteristics. However, in a well-crosslinked sample of PE/EPDM/EVA/CB, room temperature resistivity increased slightly, and the initially observed small NTC effect practically vanished. Crosslinking was thus found to eliminate the NTC effect and enhance the PTC intensity and the electrical reproducibility of the composites. Apparently a crosslinked matrix traps the CB particles, allowing them to redistribute during the movement and expansion of the matrix at high temperatures, but returning them to their original positions when the composite is cooled. This stabilizes the PTC behaviour, eliminates the NTC phenomenon, and improves the reproducibility of the resistivity behaviour. However, in another study [19], elimination of the NTC effect was achieved by using a very high viscosity semi-crystalline polymer such as UHMWPE as one of the blend components.

1.3 Objectives of the study

- Investigate the effect of a medium-soft Fischer-Tropsch paraffin wax (M3 wax), γ-irradiation and Zn metal powder as second filler on the thermo-electrical behaviour of polyolefin/CB composites. CB (activated charcoal) powder was chosen as the main filler due to its low cost and relatively good conductive properties. LDPE, HDPE and iPP were used as semi-crystalline matrices due to their wide utilization and differences in morphologies and properties.
- Study the thermal properties of the composites using differential scanning calorimetry (DSC) in order to understand the influence of the presence and amount of filler on the melting temperatures and enthalpies of the polymers in the composites.
- Establish the morphologies of the composites by studying the phase separation, continuity, and interfacial adhesion of the blend and composite components by using polarizing optical microscopy (POM) and scanning electron microscopy-energy dispersive X-ray spectroscopy (SEM-EDS).
- Determine the toughness of the composites through impact testing in order to establish their resilience during application.
- Determine the viscoelastic properties of the composites by analyzing the effect of the filler and blending on molecular relaxation processes such as the glass transition and other secondary transitions, as well as intrinsic mechanical properties such as elastic modulus, viscous modulus and damping coefficient (tan δ) of the polyolefins.

- ❖ Study the effect of CB content (12 and 22 vol.%) and blending on the room temperature resistivity, PTC intensity and switching temperature of the composites.
- ❖ Check the influence of γ-irradiation on the room temperature resistivity, PTC intensity, NTC intensity and electrical stability of the materials.
- ❖ Compare the hybrid 12CB/10Zn filler with neat 22CB by studying the effect Zn has on the resistivity behavior of the composites.

1.4 References

[1] M.-Y. Jeong, B.-Y. Ahn, S.-K. Lee, W.-K. Lee, N.-J. Jo. Antistatic coating material consisting of poly (butylacrylate-co-styrene) core-nickel shell particle. Transactions of Nonferrous Metals Society of China 2009; 19:119-123.

[2] P. Bajaj, A.P. Gupta, N. Ojha. Antistatic and hydrophilic synthetic fibers: A critique. Journal of Macromolecular Science 2000; 40:105-138.
DOI: 10.1081/MC-100100581

[3] K. Hausmann. Permanent antistatic agent offers long term performance for films and containers. Plastics, Additives and Compounding 2007; 9:40-42.

[4] Y. Xi, H. Ishikawa, Y. Bin, M. Matsuo. Positive temperature coefficient effect of LMWPE–UHMWPE blends filled with short carbon fibers. Carbon 2004; 42:1699-1706.
DOI: 10.1016/j.carbon.2004.02.027

[5] Y. Wan, C. Xiong, J. Yu, D. Wen. Effect of processing parameters on electrical resistivity and thermo-sensitive properties of carbon-black/styrene-butadiene-rubber composite membranes. Composites Science and Technology 2005; 65:1769-1779.
DOI: 10.1016/j.compscitech.2005.03.006

[6] M.-K. Seo, K.-Y. Rhee, S.-J. Park. Influence of electro-beam irradiation on PTC/NTC behaviours of carbon blacks/HDPE conducting polymer composites. Current Applied Physics 2011; 11:428-433.
DOI: 10.1016/j.cap.2010.08.013

[7] J.-M. Sansiñena, J.B. Gao, H.-L. Wang. High-performance, monolithic polyaniline electrochemical actuators. Advanced Functional Materials 2003; 13:703-709.
DOI: 10.1002/adfm.200304347

[8] W. Thongruang, R.J. Spontak, C.M. Balik. Bridged double percolation in conductive polymer composites: An electrical conductivity, morphology and mechanical property study. Polymer 2002; 43:3717-3725.
PII: S0032-3861 (02) 00180-5

[9] J.-C. Huang. Review: Carbon black filled conducting polymers and polymer blends. Advances in Polymer Technology 2002; 21:299–313.

[10] Y. Song, Q. Zheng. Conduction stability of high-density polyethylene/carbon black composites due to electric field action. European Polymer Journal 2005; 41:2998-3003.
DOI: 10.1016/j.eurpolymj.2005.04.043

[11] G.X. Mao, A.F. Zhu. Enhanced electrically conductive polypropylene/nano carbon black composite. Polymer-Plastics Technology and Engineering 2012; 51:1073-1076.
DOI: 10.1080/03602559.2012.679380

[12] G.D. Liang, S.C. Tjong. Electrical properties of low-density polyethylene/multiwalled carbon nanotube nanocomposites. Materials Chemistry and Physics 2006; 100:132–137.
DOI: 10.1016/j.matchemphys.2005.12.021

[13] M. Narkis, A. Ram, F. Flashner. Electrical properties of carbon black filled polyethylene. Polymer Engineering and Science 1978; 18:649–653.

[14] M. Narkis, A. Ram, Z. Stein. Electrical properties of carbon black filled crosslinked polyethylene. Polymer Engineering and Science 1981; 21:1049–1054.

[15] M. Narkis, A. Vaxman. Resistivity behavior of filled electrically conductive crosslinked polyethylene. Journal of Applied Polymer Science 1984; 29:1639–1652.

[16] H. Tang, J.H. Piao, X.F. Chen, Y.X. Luo, S.H. Li. The positive temperature coefficient phenomenon of vinyl polymer/CB composites. Journal of Applied Polymer Science 1993; 48:1795–1800.

[17] M.-K. Seo, K.-Y. Rhee, S.-J. Park. Influence of electro-beam irradiation on PTC/NTC behaviours of carbon blacks/HDPE conducting polymer composites. Current Applied Physics 2011; 11:428-433.
DOI: 10.1016/j.cap.2010.08.013

[18] M.-G. Lee, Y.C. Nho. Electrical resistivity of carbon black-filled high-density polyethylene (HDPE) composite containing radiation cross-linked HDPE particles. Radiation Physics and Chemistry 2001; 61:75-79.
PII: S0969-806X(00)00354-6

[19] J. Feng, C.M. Chan. Double positive temperature coefficient effects of carbon black-filled polymer blends containing two semicrystalline polymers. Polymer 2000; 41:4559-4565.

PII: S0032-3861(99)00690-4

[20] D.D.L. Chung. Review: Electrical applications of carbon materials. Journal of Materials Science 2004; 39:2645-2661.

[21] J. Wind, R. Späh, W. Kaiser, G. Bohm. Metallic bipolar plates for PEM fuel cells. Journal of Power Sources 2002; 105:256-260.

[22] Y. Cohen, K. Landskron, N. Tétreault, S. Fournier-Bidoz, B. Hatton, G.A. Ozin. A silicon-silica nanocomposite. Advanced Functional Materials 2005; 15:593-602.
DOI: 10.1002/adfm.200400069

[23] G. Yang. Effect of crosslinking and field strength on the electrical properties of carbon/polyolefin composites with a large positive temperature coefficient of resistivity. Polymer Composites 1997; 18:484-491.
DOI: 10.1002/pc.10300

[24] Bueche F. A new class of switching materials. Journal of Applied Physics 1973; 44:532-533.
DOI: 10.1063/1.1661934

[25] Y. Bin, C. Xu, Y. Agari, M. Matsuo. Morphology and electrical conductivity of ultrahigh-molecular-weight polyethylene-low-molecular-weight polyethylene-carbon black composites prepared by gelation/crystallization from solution. Colloid and Polymer Science 1999; 277:452–461.

[26] Y. Bin, C. Xu, D. Zhu, M. Matsuo. Electrical properties of polyethylene and carbon black particle blends prepared by gelation/crystallization from solution. Carbon 2002; 40:195-199.
DOI: 10.1016/S0008-6223(01)00173-7

[27] C.M. Chan, C.L. Cheng, M.M.F. Yuen. Electrical properties of polymer composites prepared by sintering a mixture of carbon black and ultra-high molecular weight polyethylene powder. Polymer Engineering and Science 1997; 37:1127-1136.

[28] H.S. Mpanza, A.S. Luyt. Comparison of different waxes as processing agents for low-density polyethylene. Polymer Testing 2006; 25:436-442.
DOI: 10.1016/j.polymertesting.2006.01.008

[29] I. Krupa, A.S. Luyt. Thermal properties of uncross-linked and cross-linked LLDPE/wax blends. Polymer Degradation and Stability 2000; 70:111-117.
DOI: 10.1016/S0141-3910(00)00097-5

[30] J.A. Molefi, A.S. Luyt, I. Krupa. Comparison of LDPE, LLDPE and HDPE as matrices for phase change materials based on a soft Fischer–Tropsch paraffin wax. Thermochimica Acta 2010; 500:88-92.

DOI: 10.1016/j.tca.2010.01.002

[31] S.P. Hlangothi, I. Krupa, V. Djoković, A.S. Luyt. Thermal and mechanical properties of cross-linked and uncross-linked linear low-density polyethylene–wax blends. Polymer Degradation and Stability 2003; 79:53-59.
PII: S0141-3910(02)00238-0

[32] I. Krupa, G. Miková, A.S. Luyt. Phase change materials based on low-density polyethylene/paraffin wax blends. European Polymer Journal 2007; 43:4695-4705.
DOI: 10.1016/j.eurpolymj.2007.08.022.

[33] I. Krupa, A.S. Luyt. Physical properties of blends of LLDPE and an oxidized paraffin wax. Polymer 2001; 42:7285-7289.
DOI: 10.1016/S0032-3861(01)00172-0

[34] T.N. Mtshali, I. Krupa, A.S. Luyt. The effect of cross-linking on the thermal properties of LDPE/wax blends. Thermochimica Acta 2001; 380:47-54.
DOI: 10.1016/S0040-6031(01)00636-0

[35] M.E. Sotomayor, I. Krupa, A. Várez, B. Levenfeld. Thermal and mechanical characterization of injection moulded high density polyethylene/paraffin wax blends as phase change materials. Renewable Energy 2014; 68:140-145.
DOI: 10.1016/j.renene.2014.01.036

[36] M.J. Hato, A.S. Luyt. Thermal fractionation and properties of different polyethylene/wax blends. Journal of Applied Polymer Science 2007; 104:2225-2236.
DOI: 10.1002/app.25494

[37] I. Krupa, G. Miková, A.S. Luyt. Polypropylene as a potential matrix for the creation of shape stabilized phase change materials. European Polymer Journal 2007; 43:895–907.
DOI: 10.1016/j.eurpolymj.2006.12.019

[38] I. Krupa, A.S. Luyt. Thermal properties of polypropylene/wax blends. Thermochimica Acta 2001; 372:137-141.
DOI: 10.1016/s0040-6031(01)00450-6

[39] T.N. Mtshali, C.G.C.E Van Sittert, V. Djoković, A.S. Luyt. Binary mixtures of polyethylene and oxidized wax: Dependency of thermal and mechanical properties upon mixing procedure. Journal of Applied Polymer Science 2003; 89:2446-2456.
DOI: 10.1002/app.12466

[40] Y. Cai, Y. Hu, L. Song, Y. Tang, R. Yang, Y. Zhang, Z. Chen, W. Fan. Flammability and thermal properties of high density polyethylene/paraffin hybrid as a form-stable phase change material. Journal of Applied Polymer Science 2006; 99:1320-1327.
DOI: 10.1002/app.22065

[41] A. Sari. Form-stable paraffin/high density polyethylene composites as solid–liquid phase change material for thermal energy storage: Preparation and thermal properties. Energy Conversion and Management 2004; 45:2033-2042.
DOI: 10.1016/j.enconman.2003.10.022

[42] I. Krupa, A.S. Luyt. Thermal and mechanical properties of extruded LLDPE/wax blends. Polymer Degradation and Stability 2001; 73:157-161.
DOI: 10.1016/S0141-3910(01)00082-9

[43] A.S. Luyt, I. Krupa. Thermal behaviour of low and high molecular weight paraffin waxes used for designing phase change materials. Thermochimica Acta 2008; 467:117-120.
DOI: 10.1016/j.tca.2007.11.001

[44] J. Xiang, L.T. Drzal. Investigation of exfoliated graphite nanoplatelets (xGnP) in improving thermal conductivity of paraffin wax-based phase change material. Solar Energy Materials and Solar Cells 2011; 95:1811-1818.
DOI: 10.1016/j.solmat.2011.01.048

[45] S. Kim, L.T. Drzal. High latent heat storage and high thermal conductive phase change materials using exfoliated graphite nanoplatelets. Solar Energy Materials and Solar Cells 2009; 93:136-142.
DOI: 10.1016/j.solmat.2008.09.010

[46] F. Hernández-Sánchez, P.J. Herrera-Franco. Electrical and thermal properties of recycled polypropylene-carbon black composites. Polymer Bulletin 2001; 45:509-516.

[47] K. Chrissafis, K.M. Paraskevopoulos, S.Y. Stavrev, A. Docoslis, A. Vassiliou, D.N. Bikiaris. Characterization and thermal degradation mechanism of isotactic polypropylene/carbon black nanocomposites. Thermochimica Acta 2007; 465:6-17.
DOI: 10.1016/j.tca.2007.08.007

[48] W. Thongruang, R.J. Spontak, C.M. Balik. Bridged double percolation in conductive polymer composites: An electrical conductivity, morphology and mechanical property study. Polymer 2002; 43:3717-3725.
PII: S0032-3861 (02) 00180-5

[49] H. Pang, Y.-Y. Piao, Y.-Q. Tan, G.-Y. Jiang, J.-H. Wang, Z.-M. Li. Thermoelectric behaviour of segregated conductive polymer composites with hybrid fillers of carbon nanotube and bismuth telluride. Materials Letters 2013; 107:150-153.
DOI: 10.1016/j.matlet.2013.06.008

[50] G. Zheming, L. Chunzhong, W. Gengchao, Z. Ling, C. Qilin, L. Xiaohui, W. Wendong, J. Shilei. Electrical properties and morphology of highly conductive composites based

on polypropylene and hybrid fillers. Journal of Industrial and Engineering Chemistry 2010; 16:10-14.
DOI: 10.1016/j.jiec.2010.01.028

[51] F. Marcq, P. Demont, P. Monfraix, A. Peigney, C. Laurent, T. Falat, F. Courtade, T. Jamin. Carbon nanotubes and silver flakes filled epoxy resin for new hybrid conductive adhesives. Microelectronics Reliability 2011; 51:1230-1234.
DOI: 10.1016/j.microrel.2011.03.020

[52] R. Socher, B. Krause, S. Hermasch, R. Wursche, P. Pötschke. Electrical and thermal properties of polyamide 12 composites with hybrid fillers systems of multiwalled carbon nanotubes and carbon black. Composites Science and Technology 2011; 71:1053-1059.
DOI: 10.1016/j.compscitech.2011.03.004

[53] H. Yang, J. Gong, X. Wen, J. Xue, Q. Chen, Z. Jiang, N. Tian, T. Tang. Effect of carbon black on improving thermal stability, flame retardancy and electrical conductivity of polypropylene/carbon fiber composites. Composites Science and Technology 2015; 113:31-37.
DOI: 10.1016/j.compscitech.2015.03.013

[54] M.A. Milani, D. González, R. Quijada, N.R.S. Basso, M.L. Cerrada, D.S. Azambuja, G.B. Galland. Polypropylene/graphene nanosheet nanocomposites by in situ polymerization: Synthesis, characterization and fundamental properties. Composites Science and Technology 2013; 84:1-7.
DOI: 10.1016/j.compscitech.2013.05.001

[55] Y. Luo, G. Wang, B. Zhang, Z. Zhang. The influence of crystalline and aggregate structure on PTC characteristic of conductive polyethylene/carbon black composite. European Polymer Journal 1998; 34:1221-1227.
PII: S0014-3057(98)00099-8

[56] Y. Wang, H.-B. Tsai. Thermal, dynamic-mechanical, and dielectric properties of surfactant intercalated graphite oxide filled maleated polypropylene nanocomposites. Journal of Applied Polymer Science 2012; 123:3154–3163.
DOI: 10.1002/app.34976

[57] S. Balabanov, K. Krezhov. Electrical conductivity and electrostatic properties of radiationally modified polymer composites with carbon black. Applied Physics 1999; 32:2573–2577.
PII: S0022-3727(99)96442-2

[58] I. Mironi-Harpazi, M. Narkis. Thermoelectric behavior (PTC) of carbon black containing TPX/UHMWPE and TPX/XL-UHMWPE blends. Polymer Physics 2001; 39:1415-1428.

[59] W.-L. Cheng, W.-F. Wu, J.-L. Song, Y. Liu, S. Yuan, N. Liu. A new kind of shape-stabilized PCMs with positive temperature coefficient (PTC) effect. Energy Conversion and Management 2014; 79:470-476.
DOI: 10.1016/j.enconman.2013.12.053

[60] W. Mhike, W.W. Focke, J.P. Mofokeng, A.S. Luyt. Thermally conductive phase-change materials for energy storage based on low-density polyethylene, soft Fischer-Tropsch wax and graphite. Thermochimica Acta 2012; 527:75-82.
DOI: 10.1016/j.tca.2011.10.008

[61] Q.-H. Zhang, D.-J. Chen. Percolation threshold and morphology of composites of conducting carbon black/polypropylene/EVA. Journal of Materials Science 2004; 39:1751-1757.
DOI: 10.1023/B:JMSC.0000016180.42896.0f

[62] J.A. Molefi, A.S. Luyt, I. Krupa, Investigation of thermally conducting phase change materials based on polyethylene/wax blends filled with copper particles. Journal of Applied Polymer Science 2010; 116:1766-1774.
DOI: 10.10022/app.31653

[63] Y. Xi, H. Ishikawa, Y. Bin, M. Matsuo. Positive temperature coefficient effect of LMWPE–UHMWPE blends filled with short carbon fibers. Carbon 2004; 42:1699-1706.
DOI: 10.1016/j.carbon.2004.02.027

[64] W.-L. Cheng, S. Yuan, J.-L. Song. Studies on preparation and adaptive thermal control performance of novel PTC (positive temperature coefficient) materials with controllable curie temperatures. Energy 2014; 74:447-454.
DOI: 10.1016/j.energy.2014.07.009

CHAPTER TWO

MATERIALS AND METHODS

2.1 Materials

Low-density polyethylene (LDPE) was supplied in pellet form by Sasol Polymers, Johannesburg, South Africa. It has a melt flow index (MFI) of 7 g/10 min (ASTM D-1238) and a molecular weight of 96 000 g mol^{-1}. It has a density of 0.918 g cm^{-3} and a melting point of 110 °C.

High-density polyethylene (HDPE) was supplied in pellet form by Safripol, Sasolburg, South Africa. It has a melt flow index (MFI) of 2 g/10 min (ISO 1133), a molecular weight of 230 489 g mol^{-1}, a density of 0.956 g cm^{-3} and a melting point of 134 °C.

Isotactic polypropylene (iPP) was supplied in pellet form by Sasol Polymers, Johannesburg, South Africa. It has a melt flow index (MFI) of 12g/10 min (230 °C/2.16 kg), a molecular weight of 399 000 g mol^{-1}, a density of 0.9 g cm^{-3} and melting point of 165 °C.

Medium-soft Fischer-Tropsch paraffin wax (M3 wax) was supplied in powder form by Sasol Wax, Johannesburg, South Africa. It consists of approximately 99% of straight-chain hydrocarbons and a few branched chains. It has an average molar mass of 440 g mol^{-1} and a carbon distribution between C15 and C78. Its density is 0.90 g cm^{-3} and it has a melting point range of ~40-60 ºC.

Carbon black (activated charcoal) was supplied by Minema Chemicals, Northcliff, South Africa. The particles have an ash content of 2%, moisture content of < 15%, and particle sizes of 7-75 μm.

Zinc metal was supplied in powder form by Merck Chemicals, Wadeville, South Africa. The metal particles are < 150 μm in size and their purity is 99.995%.

2.2 Methods

2.2.1 Sample preparation

It is common knowledge that carbon blacks (CBs) readily absorb moisture from the atmosphere. Therefore, prior to sample preparation, the activated charcoal powder was dried in an oven at 120 °C for 24 hours to eliminate any traces of humidity and to avoid the formation of lumps.

The composites and blend composites were prepared *via* melt compounding with the aid of a Brabender Plastograph with a 55 cm^3 internal mixer. CB composites with 12 (12CB) and 22 (22CB) vol.% (~25 and 40 wt.%, respectively) content, as well as 12 vol.% CB/10 vol.% Zn (12CB/10Zn) hybrid composites, were prepared while the polyolefins were blended with wax in fixed 90/10 volume ratios. Tables 2.1 and 2.2 provide the different compositions and proportions for the composites as well as the blend composites. The mixing was conducted for 15 minutes at a rotor speed of 50 rpm at 140, 160 and 190 °C for LDPE, HDPE and iPP respectively. For the composites, the polymer was first fed into the heated mixer, followed by the addition of the filler 5 minutes later, whereas for the blend composites, the filler was added into the mixing chamber 5 minutes after the addition of the mechanically pre-mixed blend components. The samples were then melt-pressed at the same temperature for 5 minutes under 50 kPa using a hydraulic melt-press. The resulting square sheets were allowed to slowly cool to room temperature between two aluminium plates. The test samples were then cut accordingly for various analyses.

2.2.2 Sample analysis

2.2.2.1 Scanning electron microscopy – energy-dispersive X-ray spectroscopy (SEM-EDS)

SEM is a microscopy technique in which a high-energy beam of electrons is scanned across a sample's surface in a vacuum chamber in a raster scan pattern. When the electrons strike the sample, a variety of signals, in the form of either X-ray fluorescence, secondary or back-scattered electrons, are generated [1]. Interaction of the primary beam with atoms in the sample causes shell transitions which result in the emission of an X-ray. The emitted X-ray

has an energy characteristic of the parent element. Detection and measurement of the energy permits elemental analysis in EDS.

Table 2.1 Volume percentages of samples for the preparation CB composites

Sample	Vol.% LDPE	Vol.% Wax	Vol.% CB
LDPE/12CB	88	0	12
LDPE/22CB	78	0	22
LDPE/wax/12CB	80	8	12
LDPE/wax/22CB	70	8	22
	Vol.% HDPE	**Vol.% Wax**	**Vol.% CB**
HDPE/12CB	88	0	12
HDPE/22CB	78	0	22
HDPE/wax/12CB	80	8	12
HDPE/wax/22CB	70	8	22
	Vol.% iPP	**Vol.% Wax**	**Vol.% CB**
iPP/12CB	88	0	12
iPP/22CB	78	0	22
iPP/wax/12CB	80	8	12
iPP/wax/22CB	70	8	22

Table 2.2 Volume percentages of samples for the preparation of 12CB/10Zn hybrid composites

Sample	Vol.% LDPE	Vol.% Wax	Vol.% CB	Vol.% Zn
LDPE/12CB/10Zn	78	0	12	10
LDPE/wax/12CB/10Zn	70	8	12	10
	Vol.% HDPE	**Vol.% Wax**	**Vol.% CB**	**Vol.% Zn**
HDPE/12CB/10Zn	78	0	12	10
HDPE/wax/12CB/10Zn	70	8	12	10
	Vol.% iPP	**Vol.% Wax**	**Vol.% CB**	**Vol.% Zn**
iPP/12CB/10Zn	78	0	12	10
iPP/wax/12CB/10Zn	70	8	12	10

In SEM, the nature of the sample determines the preparation of the sample, since appropriate samples may be examined directly with little or no prior preparation. Unfortunately, most polymers present specific problems making them inappropriate. Therefore proper sample preparation is necessary prior to characterization, and these include plasma etching, conductive coatings through evaporation or sputtering and chemical etching methods [2-3].

SEM analyses for this study were carried out using a TESCAN Vega 3 scanning electron microscope with an Oxford X-Max^n energy-dispersive X-ray spectroscope. Samples were frozen in liquid nitrogen, fractured by simply breaking the specimen into an appropriate size to fit the specimen chamber, and then mounted onto the holder. The analysis was done at room temperature and since the samples in this study are electrically (semi) conductive, the fractured samples were not coated prior to recording the SEM-EDS images.

2.2.2.2 Differential scanning calorimetry (DSC)

DSC is a thermo-analytical technique that provides quantitative information on thermal transitions in materials, especially polymers. These are the changes that occur within a polymer when it is either heated or cooled at a controlled rate. DSC measures the heat required to maintain the same temperature in the sample and an appropriate reference material during controlled heating. DSC can be used to measure the temperatures, enthalpies and changes in heat capacity of physical transitions such as melting, crystallization, glass transition, degradation, dehydration, decomposition, polymer curing, glass formation and oxidative attack [2,4-10].

The DSC analyses were performed using a Perkin Elmer DSC6000 differential scanning calorimeter under nitrogen (N_2) atmosphere (flow rate of 20 ml min^{-1}). The instrument was computer-controlled and the peak analyses were done using Pyris software. The instrument was calibrated using the onset temperatures of melting of indium and zinc standards, as well as the melting enthalpy of indium. The samples (mass range 5-10 mg) were sealed in aluminium pans and heated from 20 to 190 °C at a heating rate of 10 °C min^{-1}, and cooled under the same conditions. The same conditions were used for heating the samples in the second scan. The peak temperatures of melting and crystallization, as well as the melting and crystallization enthalpies, were determined from the cooling and second heating scans to eliminate the effects of thermal history. All the DSC measurements were repeated three times

for each composition. The temperatures and enthalpies are reported as average values with standard deviations.

2.2.2.3 Dynamic mechanical analysis (DMA)

DMA provides valuable data on the viscoelastic properties of materials, particularly polymers. Viscoelasticity describes the time-dependent mechanical properties which in limiting cases can behave as either elastic solids or viscous liquids. The basic principle is the application of an oscillating force to a sample while heating or cooling it over a temperature range, and analysing the material's response to that force. The dynamic response of the material can be divided into two characteristic quantities: the elastic and viscous parts. The former defines the energy stored in the system, whereas the latter describes the energy dissipated during the process. The damping coefficient (tan δ), which is the ratio of the loss to storage modulus, measures the internal friction of the material and indicates the amount of energy lost in the material as dissipated heat.

DMA can be used to study molecular relaxation processes such as the glass transition and other secondary transitions. Flow, as well as intrinsic mechanical properties such as elastic modulus (storage modulus, E'), viscous modulus (loss modulus, E"), and damping coefficient (tan δ) as a function of time, temperature, or frequency can be determined.

The dynamic mechanical properties of the composites in this work were studied using a Perkin Elmer Diamond DMA. The settings for the analyses were as follows:

Frequency	1 Hz
Amplitude	20 μm
Temperature range	-120 to +100 ºC
Temperature program mode	Ramp
Measurement mode	Compression
Heating rate	3 ºC min^{-1}
Preloading force	0.02 N
Disc thickness	1.4 – 1.6 mm
Disc diameter	10 mm

2.2.2.4 Electrical properties

Electrical resistivity describes the ratio of the applied voltage to the measured current. It quantifies a material's capacity to conduct, or alternatively resist the flow of electric charge. Promoting electrons from the valence band into the conduction band is a thermally activated process, and therefore, in conductive polymer composites (semiconductors), as temperature increases, the electrons in the valence band will gain energy and go into the higher energy levels in the conduction band where they become charge carriers. This facilitates conduction and the effective conductivity of the semiconductor is increased. This temperature-dependent behaviour is characteristic of conductivity of semiconductors, and it is observed from ambient to the verge of switching.

Samples in the form of discs were cut from the central parts of the melt-pressed sheets. Since conductive lining on both sides of the test samples is required for good contact with the electrodes, the surfaces of the samples were made conductive using soft graphite and volume resistivity (R) was measured in the thickness direction of the samples. The electrical measurements were performed using a Keithley 2401 ampere-meter at a constant electric field (E) application by measuring current (I) as a function of temperature (T). Specific resistivity (R_0) of the samples was calculated by taking the geometry of the samples into account using the equation: $R_0 = RA/l$, where R is the resistance of the sample, A is the cross sectional area and l is the length (thickness) of the sample. $R = V/I$, where V is the applied voltage and I the measured current, and $A = \pi r^2$ where π is a constant and r is the radius of the disc. Room temperature resistivity measurements were done during 10 s of constant electric field application at 25 °C. The settings for the analyses were as follows:

Voltage	10-20 V
Electric field	10 V mm^{-1}
Heating rate	2 ºC min^{-1}
Temperature range	20-95 °C
Disc thickness	1.0-2.0 mm
Disc diameter	10 mm

2.2.2.5 Impact testing

The toughness of a material can be determined using impact testing. This technique measures a material's ability to resist high-rate loading since different materials differ in their ability to absorb energy during plastic deformation. Ductile materials can endure a high amount of plastic deformation compared to their brittle counterparts. A material's ability to resist impact is often one of the determining factors in its service life, or in the suitability of a material for a particular application. Impact testing can be categorized into two main types, the Charpy and Izod impact tests. Both these methods use the same principle to test the impact strength, which involves striking a standard specimen with a controlled weight pendulum travelling at a set speed. When the pendulum impacts the specimen, the specimen will absorb energy until it yields and the energy that is needed to fracture the sample is measured in kJ m^{-2}. In the Charpy test, the sample is placed horizontally and the hammer strikes the sample on the opposite side of the notch, while during the Izod test, the sample is placed vertically and clamped at one end just below the notch and the hammer usually hits the sample on the notched side. In this study the Charpy testing method was employed to study the impact properties of pure HDPE, its blends and composites.

A Ceast Impactor II was employed to determine the impact properties of the conductive composites and also to discover if the addition of the filler did not induce a decline in impact properties. The samples were rectangular in shape with a width of 10 mm, a thickness of 2.2-2.9 mm and a length of 80 mm, and were V-notched (2 mm deep) edgewise. The pendulum hammer was situated at an angle of 150° from the release spot, and the samples were tested at ambient temperature (usually 24 °C). Five samples from each composition were tested and the average and standard deviation values are reported.

2.3 References

[1] A. Bogner, P.H. Jouneau, G. Thollet, D. Basset, C. Gauthier. A history of scanning electron microscopy developments: Towards “Wet-STEM” imaging. Micron 2007; 38:309-401.
DOI: 10.1016/j.micron.2006.06.008

[2] B.J. Hunt, M.I. James. Polymer Characterization, 1st edition. Blackie Academic & Professional, London (1997).

[3] F. Oulevey, N.A. Burnham, G. Gremand, A.J. Kulik, H.M. Pollock, A. Hammiche, M. Reading, M. Song, D.J. Hourston. Dynamic mechanical analysis at the submicron scale. Polymer 2000; 41:3087-3092.
DOI: 10.1016/S0032-3861(99)00601-1

[4] W. Hemminger, S.M. Sarge. Definitions, nomenclature, terms and literature. In: M.E. Brown (Editor). Handbook of Thermal Analysis and Calorimetry, Volume 1. Principles and Practice. Elsevier Science, Amsterdam (1998) p.8-16.

[5] G.B. McKenna, S.L. Simon. The glass transition: Its measurement and underlying physics. In: S.Z.D. Cheng (Editor). Handbook of Thermal Analysis and Calorimetry, Volume 3. Applications to Polymers and Plastics. Elsevier Science, Amsterdam (2002) p.85-92.

[6] B. Wunderlich. Thermal Analysis of Polymeric Materials. Springer-Verlag, Berlin (2005) p.279-438.

[7] P.J. Haines. Thermal Methods of Analysis: Principles, Applications and Problems, 1st edition. Blackie Academic & Professional, London (1995).

[8] E.L. Charsley, S.B. Warrington. Thermal Analysis - Techniques and Applications. Royal Society of Chemistry, Leeds (1992).

[9] T. Hatakeyama, F.X. Quinn. Thermal Analysis: Fundamentals and Applications to Polymer Science. John Wiley & Sons, Chichester (1994).

[10] M.E. Brown. Introduction to Thermal Analysis: Techniques and Applications, 1st edition. Chapman & Hall, London (1988).

[11] D. Campbell, R.A. Pethrick, J.R. White. Polymer Characterization: Physical Techniques, 2nd edition. Stanley Thornes Ltd, London (2000).
ISBN 0-7487-4005-8

[12] J.D. Menczel, R.B. Prime. Thermal Analysis of Polymers: Fundamentals and Applications. John Wiley & Sons Inc, New Jersey (2009).
ISBN 978-0-471-76917-0

[13] S.R. Sandler, W. Karo, J.A. Bonesteel, E.M. Pearce. Polymer Synthesis and Characterization: A Laboratory Manual. Academic Press, New York (1998).
ISBN 0-12-618240-X

[14] R.K. Goyal, A.N. Tiwari, Y.S. Negi. Role of interface on dynamic modulus of high-performance poly(etherether ketone)/ceramic composites. Journal of Applied Polymer Science 2011; 121:436-444.
DOI: 10.1002/app.33684

[15] R.P. Chartoff, J.D. Menczel, S.H. Dillman. Dynamic mechanical analysis (DMA). In: J.D. Menczel, R.B. Prime (Eds.). Thermal Analysis of Polymers: Fundamentals and Applications. John Wiley & Sons, Inc., Hoboken, New Jersey (2009).

[16] H.A. Khonakdar, U. Wagenknecht, S.H. Jafari, R. Hässler, H. Eslami. Dynamic mechanical properties and morphology of polyethylene/ethylene vinyl acetate copolymers blends. Advances in Polymer Technology 2004; 23:307-315.
DOI: 10.1002/adv.20019

[17] P.V. Joseph, G. Mathew, K. Joseph, G. Groeninckx, S. Thomas. Dynamic mechanical properties of short sisal fibre reinforced polypropylene composites. Composites: Part A 2003; 34:275-290.
DOI: 10.1016/S1359-835X(02)00020-9.

[18] R. Brown. Handbook of Polymer Testing. Short-Term Mechanical Tests. Rapra Polymer Testing Series, United Kingdom (2002).
ISBN: 1-85957-324-X

[19] I.M. Ward, J. Sweeney. An Introduction to the Mechanical Properties of Solid Polymers, 2nd Edition. John Wiley & Sons Ltd, Chichester (2005).
ISBN: 9780470020371

CHAPTER THREE

RESULTS AND DISCUSSION

3.1 Morphology

Optical microscopy images (results not displayed here) showed the CB composites as black sheets, which did not give any information regarding the distribution of the filler particles. It was therefore assumed that the CB micro-particles were fairly well-dispersed throughout the polymer matrices in all the composites. In the 12CB/10Zn hybrid composites, the two fillers could not be distinguished from each other.

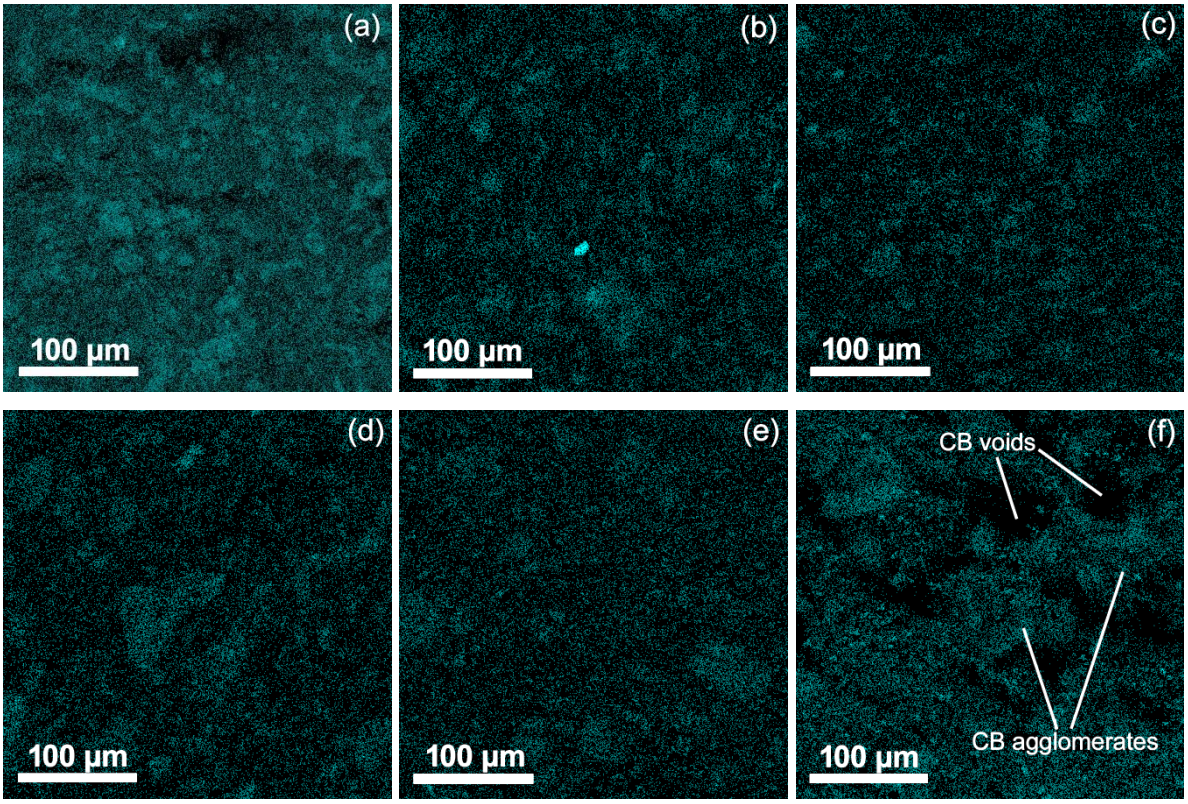

Figure 3.1 SEM-EDS images of the (a) LDPE/12CB, (b) LDPE/wax/12CB, (c) HDPE/12CB, (d) HDPE/wax/12CB, (e) iPP/12CB and (f) iPP/wax/12CB composites showing phosphorus (P) as blue dots

The SEM-EDS images clearly show the respective distributions of CB and Zn in the respective polymers and blends. CB was well-dispersed in all the polymer and blend matrices (Figure 3.1), as indicated by the dispersion of phosphorus (P) that forms part of the CB particles (the activated charcoal powder contained phosphates). However, all the pictures

show areas where CB is more concentrated, and others with almost no CB (Figure 3.1(f)). It looks as if the CB dispersion is similar in all the LDPE, HDPE and iPP composites, since their images show similar filler distributions. Differences in CB dispersion could not be linked with the type of polymer, or with the absence or presence of wax.

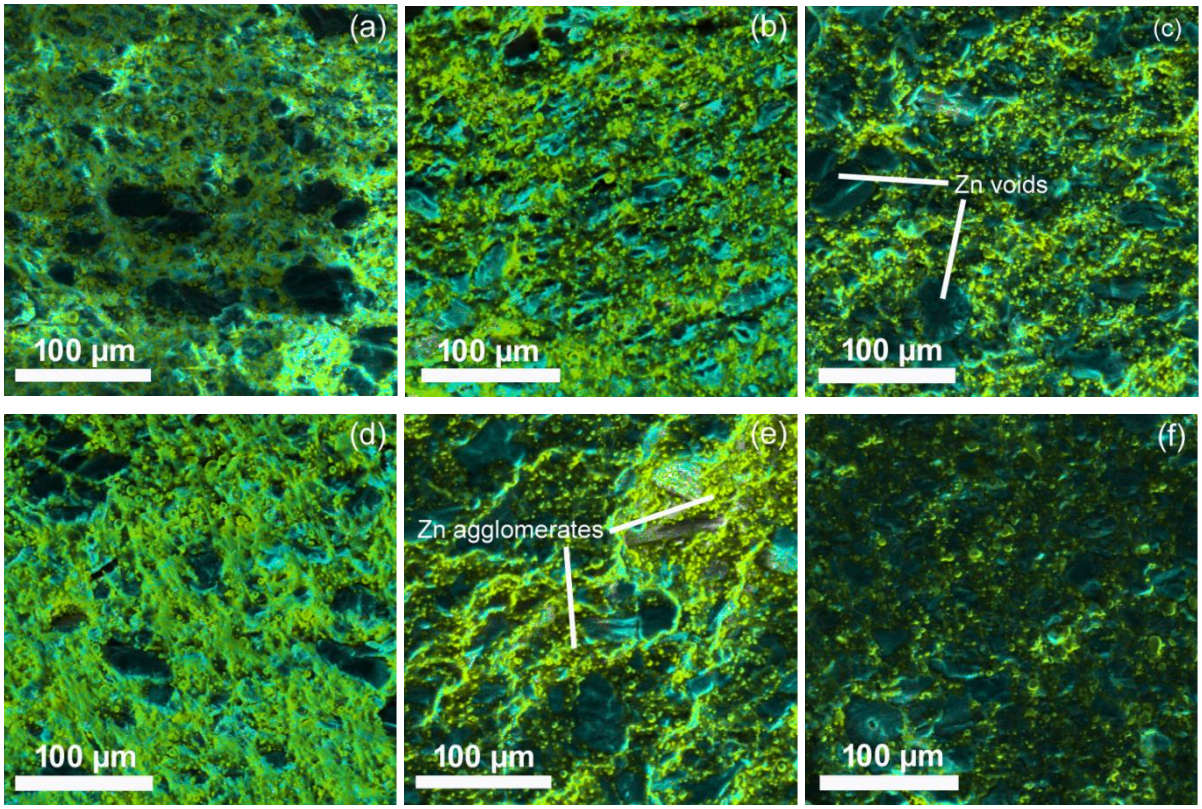

Figure 3.2 SEM-EDS layered images of the (a) LDPE/12CB/10Zn, (b) LDPE/wax/12CB/10Zn, (c) HDPE/12CB/10Zn, (d) HDPE/wax/12CB/10Zn, (e) iPP/12CB/10Zn and (f) iPP/wax/12CB/10Zn composites showing P and Zn as blue and yellow dots, respectively

Figure 3.2 presents the distributions of both CB and Zn in the hybrid composites. The images show that CB was still fairly well-dispersed, despite the presence of the metal particles in the composites. Zn was, however, randomly dispersed with clear areas that are void of Zn (Figure 3.2(c)), and agglomeration of Zn particles in other areas (Figure 3.2(e)). They also formed clear conductive pathways. Again the Zn dispersion could not be linked with the type of polymer and/or the presence of wax in the polymer matrix. The difference in the dispersions of CB and Zn in the hybrid composites suggests that there was a fairly weak interaction between the two fillers. It is possible that the metal particles could have had a stronger interaction with wax than with the matrix polymer and/or CB, which would mean that the Zn dispersed primarily in the wax. Stronger affinity between wax and copper particles has been

previously observed [1]. This could, however, not be established from the presented images in Figure 3.2.

3.2 Differential scanning calorimetry (DSC)

The DSC heating curves of the neat polymers, used in this investigation, are presented in Figure 3.3, and the values obtained from these curves are summarized in Table 3.1. The melting peak maxima were at 60, 110, 134 and 165 °C respectively for wax, LDPE, HDPE and iPP. The normalised melting enthalpies, as well as the degrees of crystallinity, were calculated with Equations 3.1 and 3.2, respectively.

$$\Delta H_m^n = \frac{Measured\ \Delta H_m}{Mass\ fraction\ of\ polymer} \quad (3.1)$$

$$X_c = \frac{\Delta H_m^n}{\Delta H_m^0} \text{ x } 100\% \quad (3.2)$$

where X_c is the degree of crystallinity, $\Delta H_m{}^n$ the normalised melting enthalpy of the specific polymer in the sample, and $\Delta H_m{}^0$ is the specific melting enthalpy of the 100% crystalline polymer. In this study, the specific melting enthalpies were taken as 293.0 and 134.9 J g^{-1} [2-4] for polyethylene and polypropylene, respectively. Based on these values, iPP had the highest crystallinity of 81.9%.

Figure 3.4 shows the DSC heating curves of the LDPE, HDPE and iPP composites filled with CB at different contents and with 12CB/10Zn. The incorporation of fillers into a polymer matrix can have two possible effects: a filler could either immobilize the polymer chains or act as a nucleating agent for the crystallization of the polymer. Chain immobilization usually leads to reduced crystallinity due to disruption of the reorientation and chain folding during crystallization, as well as lower melting temperatures as a consequence of the formation of smaller and more imperfect crystallites. On the other hand, nucleation usually gives rise to increased crystallinity and higher crystallization temperatures, since the filler particles can act as nucleating sites for the crystallization and crystal growth of a polymer. The crystallinity values decreased with an increase in CB loading in all the investigated samples (Table 3.1), which suggests lower crystallinity. This could be attributed to the immobilization of the polymer chains by the CB particles, which would suppress the crystallization process. The

presence of Zn, however, gave rise to higher crystallinities. The Zn particles obviously acted as very effective nucleation centres and have an opposite effect to that of the CB particles.

Table 3.1 Values obtained from DSC melting and crystallization data

Sample	T_m / °C	ΔH_m / J g^{-1}	ΔH_m^n / J g^{-1}	T_c / °C	X_c / %
Neat polymers/wax					
Wax	60.2 ± 0.3	173.7 ± 1.7	-	53.6 ± 0.2	59.3
LDPE	109.9 ± 1.2	73.4 ± 0.4	-	93.2 ± 1.2	25.1
HDPE	134.3 ± 0.1	210.1 ± 0.9	-	116.9 ± 0.4	71.7
iPP	164.7 ± 0.4	110.5 ± 0.8	-	113.1 ± 0.3	81.9
LDPE					
Non-irradiated LDPE composites					
LDPE/12CB	107.3 ± 0.2	53.8 ± 0.6	71.7	92.9 ± 0.3	24.5
LDPE/wax/12CB	106.5 ± 0.0	46.1 ± 1.3	68.3	92.8 ± 0.1	23.3
LDPE/22CB	105.2 ± 0.2	26.3 ± 2.2	43.8	89.9 ± 0.2	14.9
LDPE/wax/22CB	105.7 ± 0.4	27.8 ± 0.8	51.5	89.4 ± 0.3	17.6
LDPE/12CB/10Zn	106.9 ± 0.3	27.6 ± 0.3	62.6	92.7 ± 0.2	21.4
LDPE/wax/12CB/10Zn	106.5 ± 0.3	26.5 ± 0.7	66.8	92.3 ± 0.3	22.8
Irradiated LDPE composites					
LDPE/12CB	105.4 ± 1.1	46.2 ± 3.7	61.6	90.4 ± 90.4	21.0
LDPE/wax/12CB	104.9 ± 0.6	39.8 ± 2.3	59.0	91.0 ± 0.4	20.1
LDPE/22CB	103.3 ± 0.5	25.2 ± 1.1	42.0	88.3 ± 0.6	14.3
LDPE/wax/22CB	103.0 ± 0.7	24.8 ± 0.4	45.9	88.5 ± 0.6	15.7
LDPE/12CB/10Zn	105.3 ± 0.7	27.2 ± 1.3	61.7	90.0 ± 0.4	21.1
LDPE/wax/12CB/10Zn	104.9 ± 0.4	24.8 ± 1.9	62.5	90.3 ± 0.3	21.3
HDPE composites					
HDPE/12CB	134.1 ± 0.5	111.2 ± 1.1	148.3	116.8 ± 0.6	50.6
HDPE/wax/12CB	132.9 ± 0.3	118.7 ± 0.9	175.9	115.9 ± 0.2	60.0
HDPE/22CB	133.4 ± 0.6	76.0 ± 2.5	126.7	116.8 ± 0.7	43.2
HDPE/wax/22CB	132.0 ± 0.5	84.7 ± 2.8	156.9	116.1 ± 0.4	53.5
HDPE/12CB/10Zn	133.4 ± 0.4	80.8 ± 3.8	183.2	117.4 ± 0.4	62.5
HDPE/wax/12CB/10Zn	132.5 ± 0.5	74.2 ± 0.3	186.9	115.9 ± 0.7	63.8
iPP composites					
iPP/12CB	168.1 ± 0.2	70.4 ± 1.4	93.9	128.1 ± 0.1	69.6
iPP/wax/12CB	165.8 ± 0.4	77.8 ± 1.0	115.3	126.8 ± 0.2	85.5
iPP/22CB	167.6 ± 0.1	41.3 ± 2.7	68.8	131.3 ± 0.5	51.0
iPP/wax/22CB	166.1 ± 0.1	55.9 ± 3.9	103.5	129.5 ± 0.0	76.7
iPP/12CB/10Zn	168.3 ± 0.2	38.0 ± 1.9	86.2	128.5 ± 0.1	63.9
iPP/wax/12CB/10Zn	165.8 ± 0.3	39.6 ± 0.4	99.7	128.1 ± 0.2	73.9

T_m – melting peak temperature, T_c – crystallization peak temperature, ΔH_m – observed melting enthalpy, ΔH_m^n – melting enthalpy normalised with respect to LDPE/HDPE/iPP content; X_c – degree of crystallinity of LDPE/HDPE/iPP calculated from normalised enthalpy values. Values were obtained from LDPE/HDPE/iPP melting/crystallization peaks.

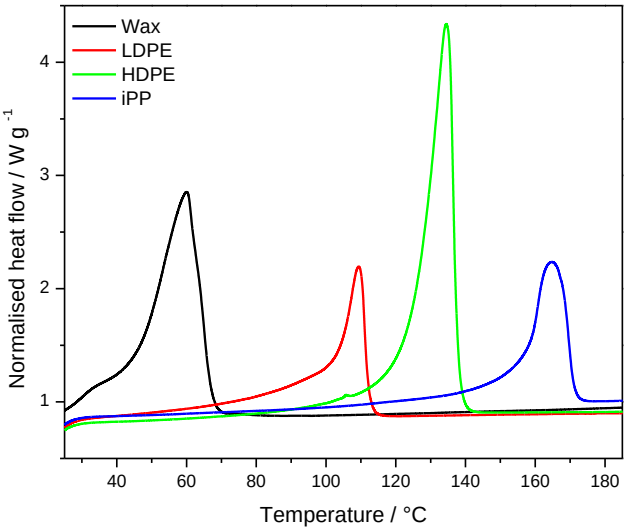

Figure 3.3 DSC heating curves of pure wax, LDPE, HDPE and iPP

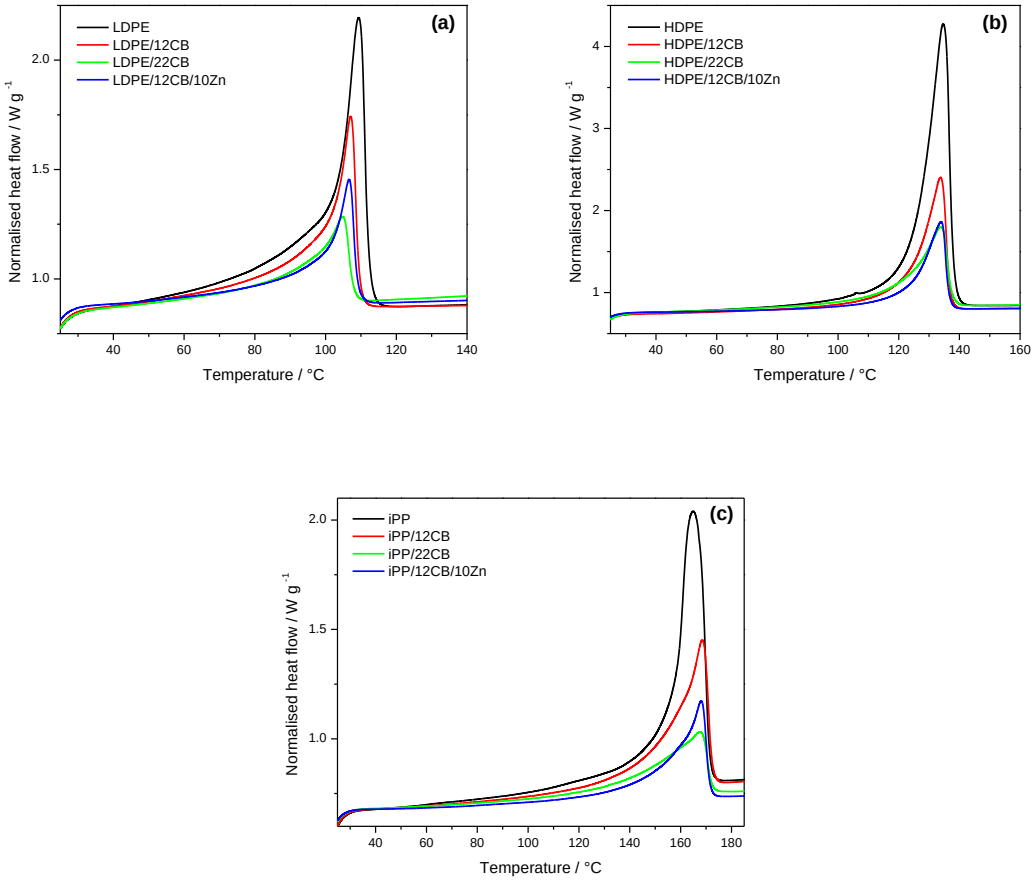

Figure 3.4 DSC heating curves of (a) LDPE, (b) HDPE, and (c) iPP and their respective composites

The melting and crystallization temperatures of LDPE and HDPE in the composites are slightly lower than those of the neat polymers (Table 3.1). This shows that the filler particles also had an effect on the crystallite sizes. In contrast, although the iPP in the composites showed lower crystallinities, the melting and crystallization occurred at slightly higher temperatures in all the composites. Although this may indicate the formation of larger crystallites [5], the differences are fairly small, and therefore it would not be justified to put too much significance to this observation.

The effect of wax in the LDPE, HDPE and iPP composites on the melting behaviour of these polymers is illustrated in Figures 3.5 to 3.7. There is a fairly strong general increase in crystallinity with the addition of wax, which counters the decrease initially observed with the addition of the filler, and this could be the result of two things: there is either a stronger interaction between the wax and the filler particles than between the polymer and the filler particles, so that the wax crystallizes on the surfaces of the filler particles and covers them, or the wax co-crystallizes with the polymer it has been blended with. If the wax covers the particles and consequently crystallizes on their surfaces, this would mean the particles are acting as nucleating agents, and this usually gives rise to a higher crystallinity. If the short wax chains co-crystallize with the polymer chains, this would also lead to increased crystallinity since the crystalline wax would contribute to the total crystallinity of the polymer. It is most likely that the latter is the reason for our observed increase in crystallinity, since there was no wax melting peak visible in any of the DSC curves of the wax-containing composites, which should have been the case if the wax on the surface of the particles would melt before the polymer. The melting and crystallization temperatures of the polymers did not significantly change in the presence of wax and look very similar within experimental error. This means that the crystallite sizes were little influenced by the presence of wax.

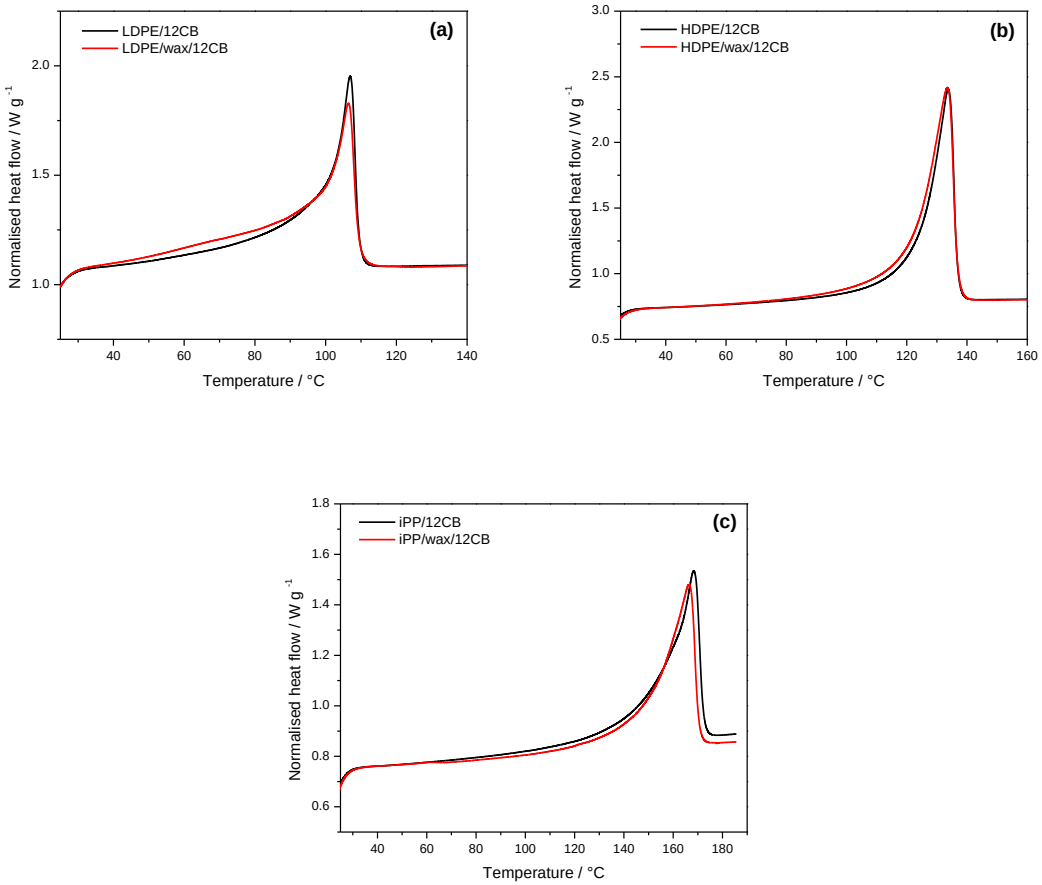

Figure 3.5 DSC heating curves of (a) LDPE/12CB, (b) HDPE/12CB, and (c) iPP/12CB showing the effect of blending

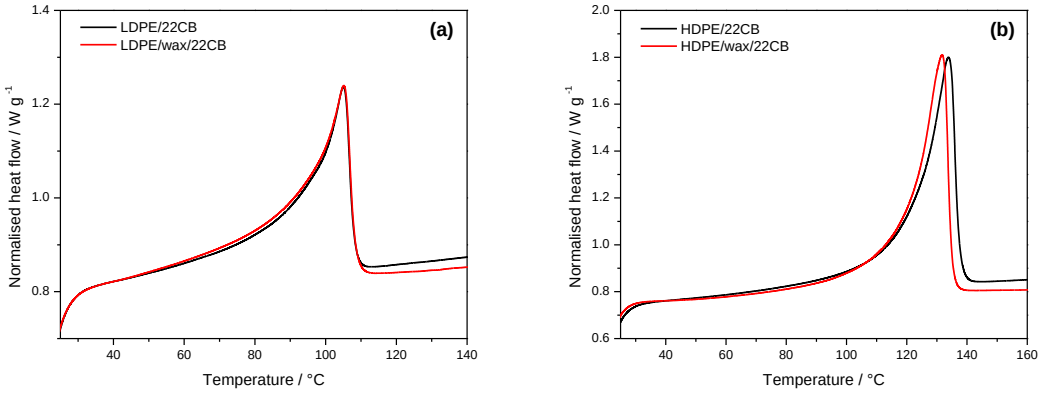

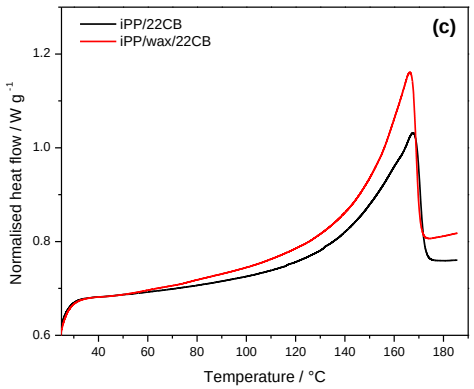

Figure 3.6 DSC heating curves of (a) LDPE/22CB, (b) HDPE/22CB, and (c) iPP/22CB showing the effect of blending

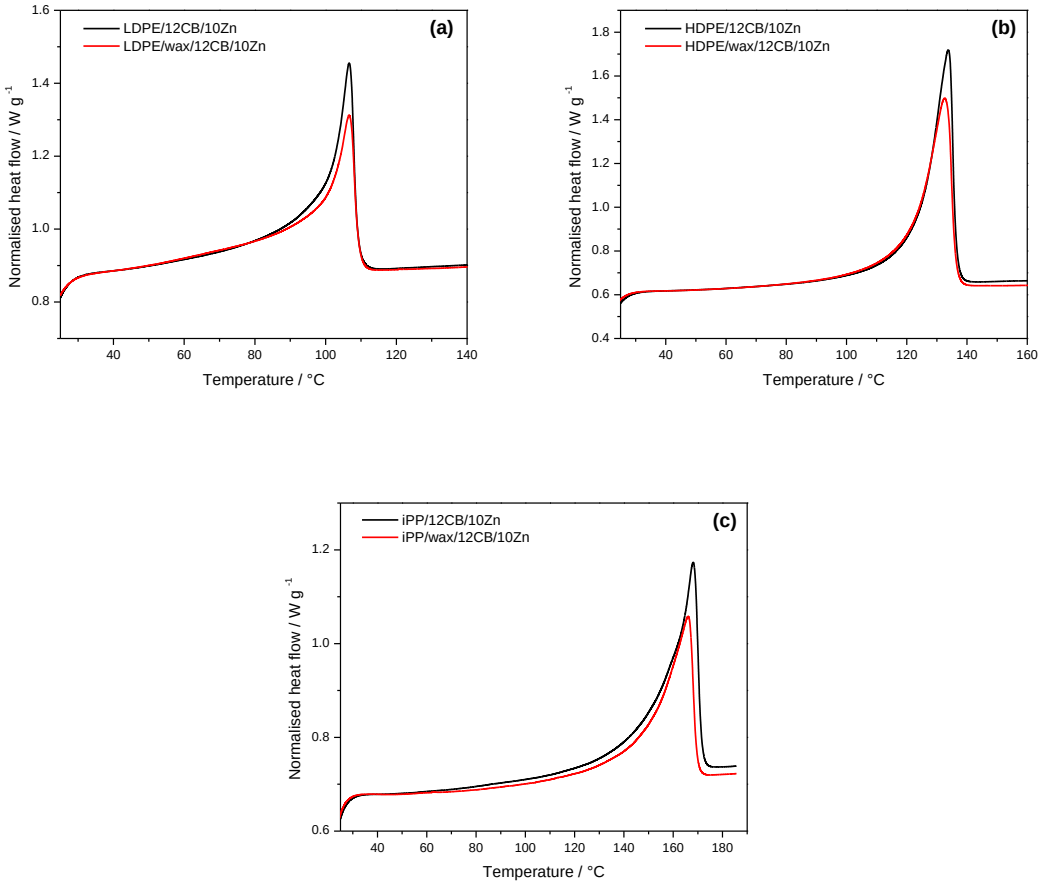

Figure 3.7 DSC heating curves of (a) LDPE/12CB/10Zn, (b) HDPE/12CB/10Zn and (c) iPP/12CB/10Zn showing the effect of blending

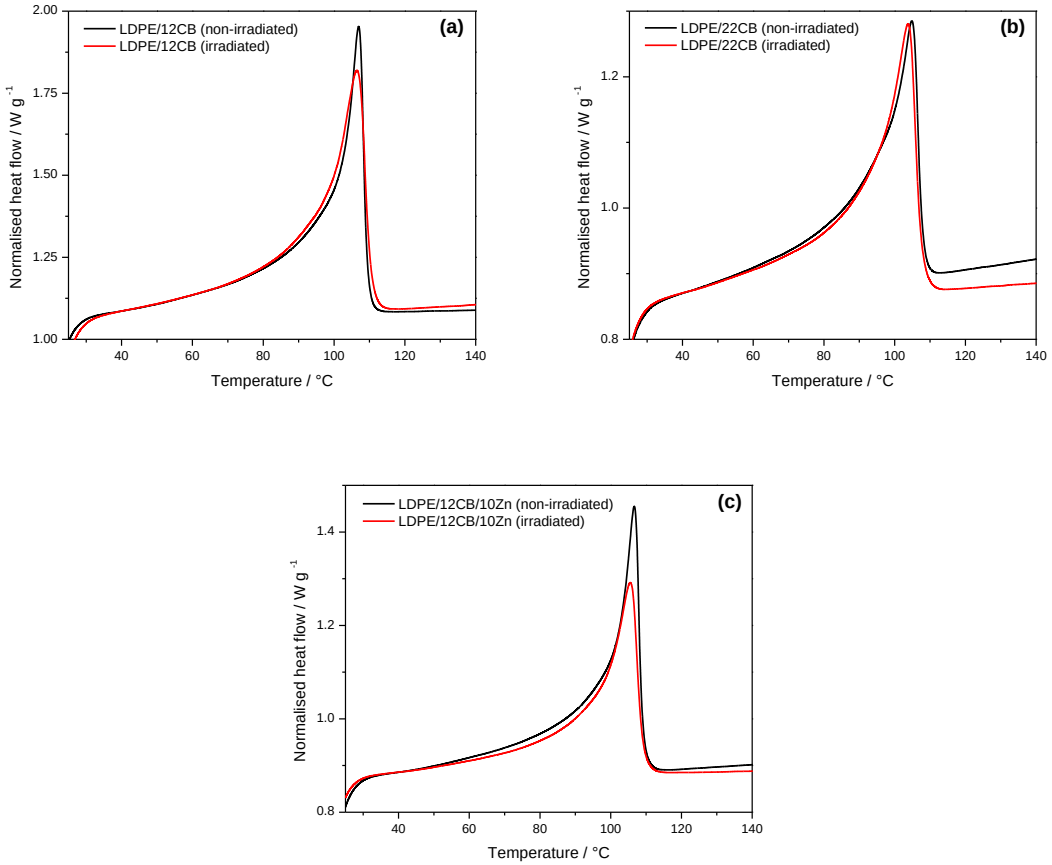

Figure 3.8 DSC heating curves of (a) LDPE/12CB, (b) LDPE/22CB, and (c) LDPE/12CB/10Zn showing the effect of irradiation

The influence of irradiation on the melting behaviour of the LDPE composites is presented in Figures 3.8 and 3.9. The investigated samples were irradiated with 100 kGy at room temperature. It is clear from the curves and the values in Table 3.1 that at a specific filler loading, the irradiated samples show lower melting and crystallization temperatures and crystallinities than the non-irradiated samples. Irradiation can have two possible effects on a polymer: it can either cause degradation through chain scission, or induce crosslinking, although a combination of the two usually prevails. If there is chain scission, there should be an increase in crystallinity, since the shorter polymer chains will more easily rearrange into a crystalline structure. On the contrary, if there is crosslinking, the polymer chains will be immobilised by the crosslinks, causing a reduction in crystallinity. It is known that the presence of crosslinks suppresses crystallization, and the three-dimensional network formed as a result of crosslinking inhibits lamellar thickening during crystallization [6-8]. Although our results may indicate that crosslinking was more dominant than chain scission because of

the observed lower crystallinities, this might not be true since the degree of crosslinking, which cannot be determined by DSC, is not known. However, we can conclude from these melting enthalpy values that the observed crystallinities are lower, probably because gamma radiation distorted the polymer crystals to a certain extent. Lower melting temperatures, which usually indicate a decrease in the average lamellar thickness, were also observed, and this could be ascribed to the effects described above. The presence of wax did not seem to have changed the influence of irradiation on the crystallinities of LDPE in the composite samples (Table 3.1), although it is quite possible that crosslinking and/or degradation of the wax could have taken place.

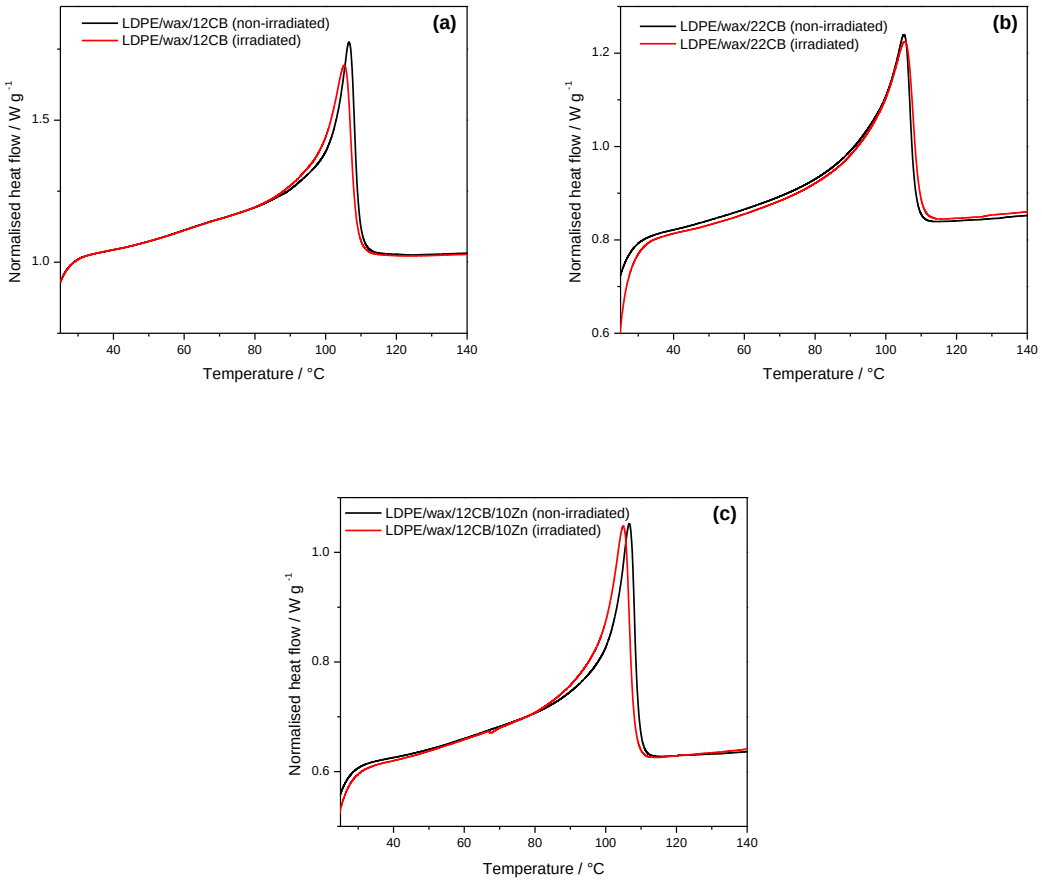

Figure 3.9 DSC heating curves of (a) LDPE/wax/12CB, (b) LDPE/wax/22CB, and (c) LDPE/wax/12CB/10Zn showing the effect of irradiation

3.3 Dynamic mechanical analysis (DMA)

Figure 3.10 shows the DMA curves of LDPE and its composites, and the storage modulus values of the investigated samples at low and high temperatures are summarized in Table 3.2.

The storage modulus values of the composites are significantly higher than those of neat LDPE (Figure 3.10(a)) throughout the investigated temperature range, and this is attributed to the presence of rigid CB and Zn particles that impart stiffness to the samples. There are, however, fairly small differences in the modulus values between the different composites.

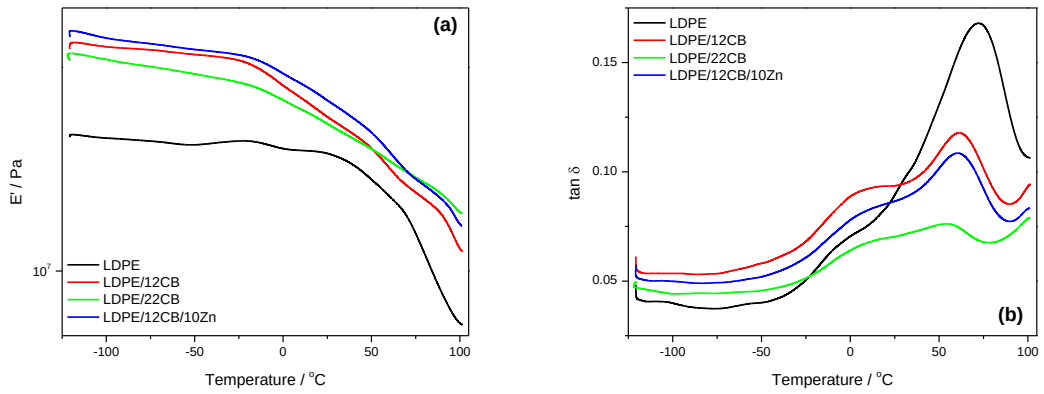

Figure 3.10 DMA results for LDPE and the non-irradiated LDPE/12CB, LDPE/22CB and LDPE/12CB/10Zn composites

Table 3.2 DMA elastic modulus values of the investigated samples

Sample	Non-irradiated		Irradiated	
	10^{-7} E' / Pa (-75 °C)	10^{-7} E' / Pa (75 °C)	10^{-7} E' / Pa (-75 °C)	10^{-7} E' / Pa (75 °C)
LDPE	2.79	1.33	-	-
LDPE/12CB	5.75	1.86	6.31	1.78
LDPE/wax/12CB	3.49	0.54	6.10	1.75
LDPE/22CB	5.03	2.09	4.98	2.26
LDPE/wax/22CB	4.37	2.39	4.61	2.02
LDPE/12CB/10Zn	6.03	2.07	6.40	2.01
LDPE/wax/12CB/10Zn	6.27	1.90	6.07	2.09

The damping or loss factor curve of neat LDPE usually shows three transitions or relaxations before melting, which are termed α, β and γ in order of decreasing temperature. The β-relaxation is usually associated with motions within the amorphous regions, while the α-relaxation is characteristic of the motions in the crystalline phase of the polymer [9,10]. The γ-transition, which usually occurs around -120 °C, is not clearly visible from our loss factor

curves (Figure 3.10(b)), since its onset is outside the temperature range used in our analysis. The β-transition, which can be regarded as the glass transition of LDPE, is observed at around -15 °C, while an intense, broad α-transition, which can be regarded as a combination of the movement of larger chain segments in the amorphous phase and the slippage between crystallites [11], can be seen at approximately 65 °C. The temperatures at which these transitions occur shifted only slightly in the presence of the fillers, but a significant decrease in the intensity of the α-transition was observed. Since this transition is related to the crystalline phase of the polymer, a decrease in its intensity can be attributed to the decreased crystallinity of the LDPE (Table 3.1), and to the immobilisation of the polymer chains by the filler particles in the inter-crystalline amorphous regions. This effect becomes more prominent with increasing CB content, but the presence of Zn did not significantly influence the intensity of this transition. This corresponds well with our DSC observations, and is probably the result of a stronger interaction between the CB particles and the matrix.

The DMA results for the different LDPE composites in the absence and presence of wax are compared in Figures 3.11 to 3.13. A clear decrease in the storage modulus is observed in the presence of wax in the 12 vol.% CB containing composites (Table 3.2), and this can be ascribed to the shorter wax chains, which induce softening of the amorphous phase of LDPE. This effect, however, is more pronounced at +75 °C since the wax is in the molten state at this temperature. At 22 vol.% CB, the differences in storage moduli are fairly small, since the stiffness is largely determined by the amount of CB in the sample. The wax therefore seems to have little influence because of the relatively large amount of CB in the sample. This behaviour is also observed in the 12CB/10Zn composites, and can be explained in the same way. The damping or loss factor curves show both the β- and α-transitions in the investigated temperature range. Addition of wax did not have any significant effect on the glass transition temperatures, irrespective of the filler loading. It obviously has little influence on the mobility of the chains in the amorphous regions. In contrast, the presence of wax did influence the high-temperature α-relaxation, which shifted to slightly higher temperatures and also increased in intensity. Although wax melts in the same temperature range as the observed α-transition, the wax melting could not have significantly contributed to the observed increase in intensity of the transition in this temperature range. Our DSC results (section 3.2) indicate that the wax co-crystallizes with LDPE, and therefore, it could not melt before the LDPE lamellae started to melt. However, the amorphous phase of LDPE became softer because of the presence of wax.

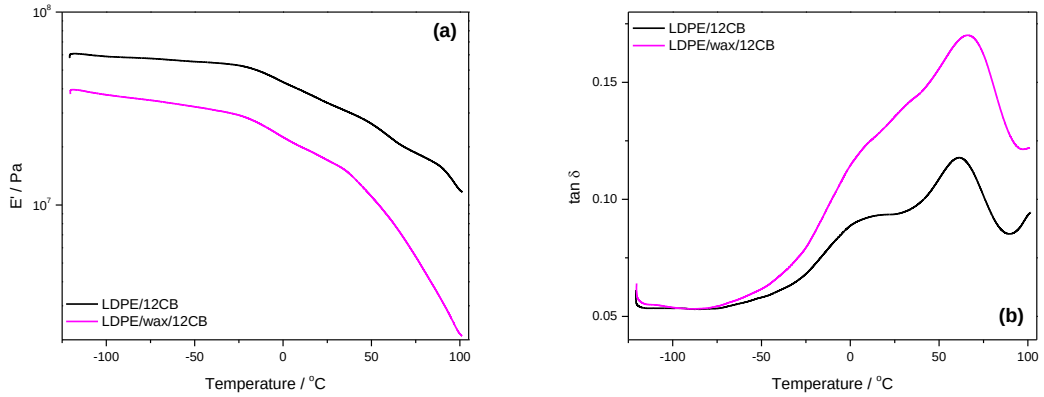

Figure 3.11 DMA results for non-irradiated LDPE/12CB and LDPE/wax/12CB composites

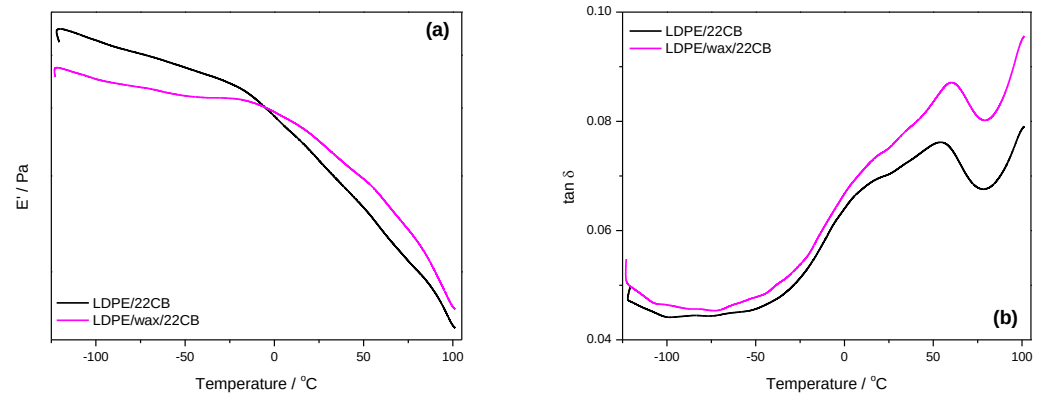

Figure 3.12 DMA results for the non-irradiated LDPE/22CB and LDPE/wax/22CB composites

Figures 3.14 to 3.19 show the influence of irradiation on the DMA curves of the LDPE/CB composites. There are generally fairly small differences in the storage modulus curves of the non-irradiated and irradiated samples, which could be an indication that irradiation had little or no effect on the stiffness of the materials. The irradiated 12 vol.% CB and wax-containing composite does not show the marked drop in storage modulus as the corresponding non-irradiated composite, probably because the wax was linked to the polymer through the formation of crosslinks [12]. Therefore, since the crosslinking binds the polymer and wax together, the effect of the softness of the wax will be less prominent. However, crosslinking and the presence of wax did not seem to have a significant influence on the modulus in the 22CB and 12CB/10Zn containing composites due to the much larger amount of filler in the samples. It therefore seems as if the radiation crosslinking, if any, had little effect on the dynamic mechanical behaviour of the composites. The exception is LDPE/wax/12CB, but this

sample may have to be re-analysed to confirm the observed behaviour. This was unfortunately not possible in the available time frame for the finalisation of this dissertation, but will be done before writing a publication.

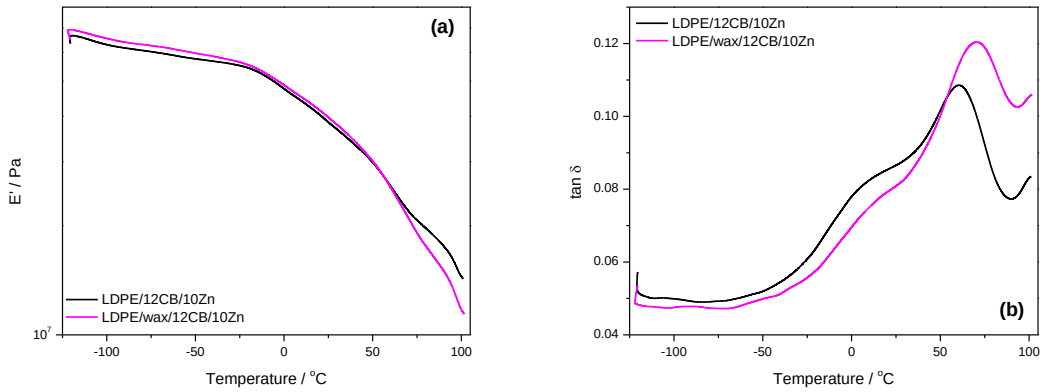

Figure 3.13 DMA results for the non-irradiated LDPE/12CB/10Zn and LDPE/wax/12CB/10Zn composites

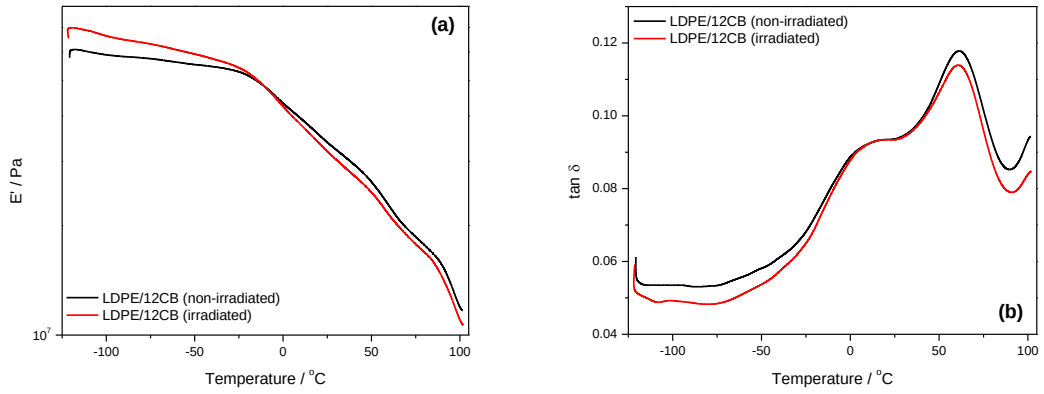

Figure 3.14 Effect of irradiation on the DMA results of LDPE/12CB composites

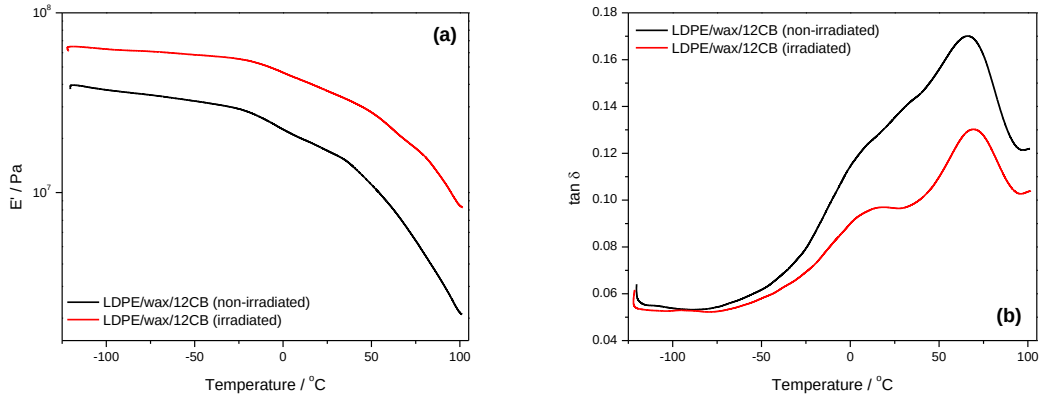

Figure 3.15 Effect of irradiation on the DMA results of LDPE/wax/12CB composites

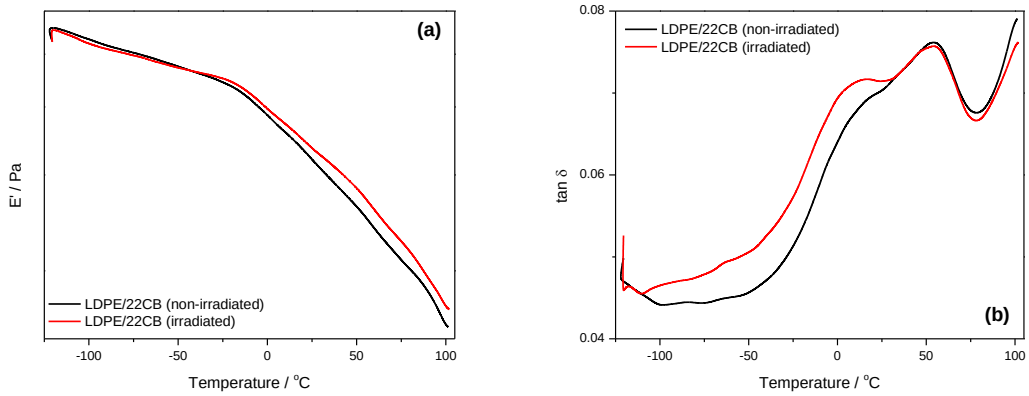

Figure 3.16 Effect of irradiation on the DMA results of LDPE/22CB composites

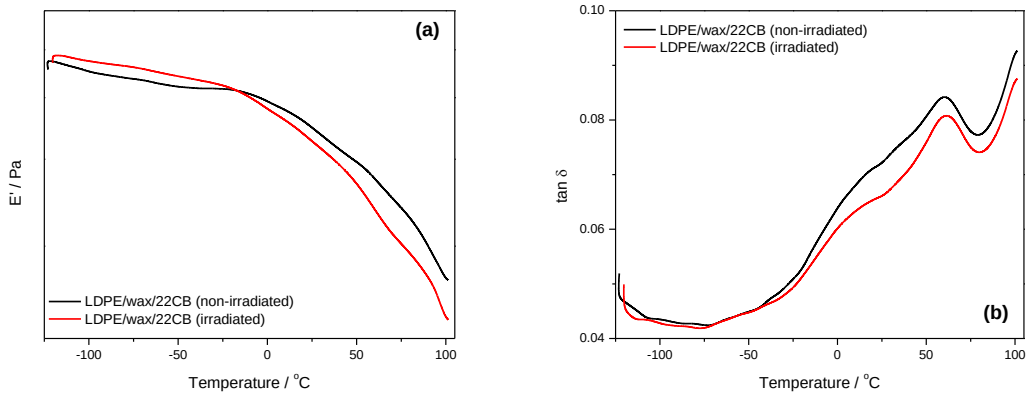

Figure 3.17 Effect of irradiation on the DMA results of LDPE/wax/22CB composites

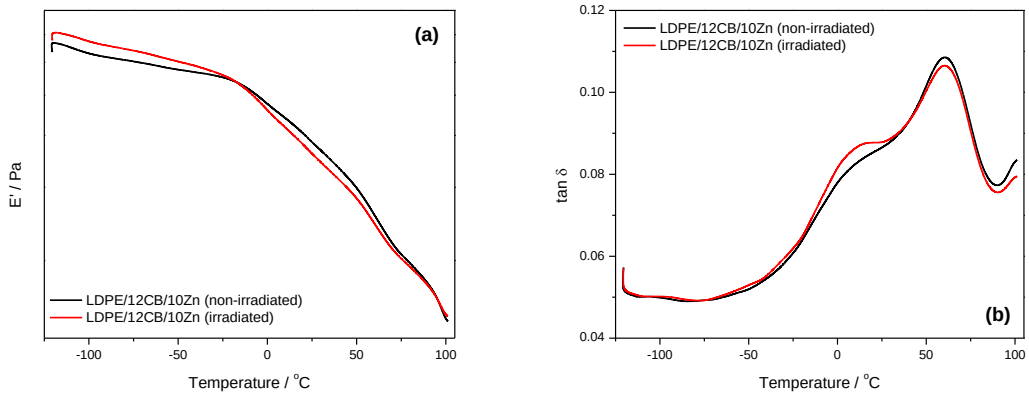

Figure 3.18 Effect of irradiation on the DMA results of LDPE/12CB/10Zn composites

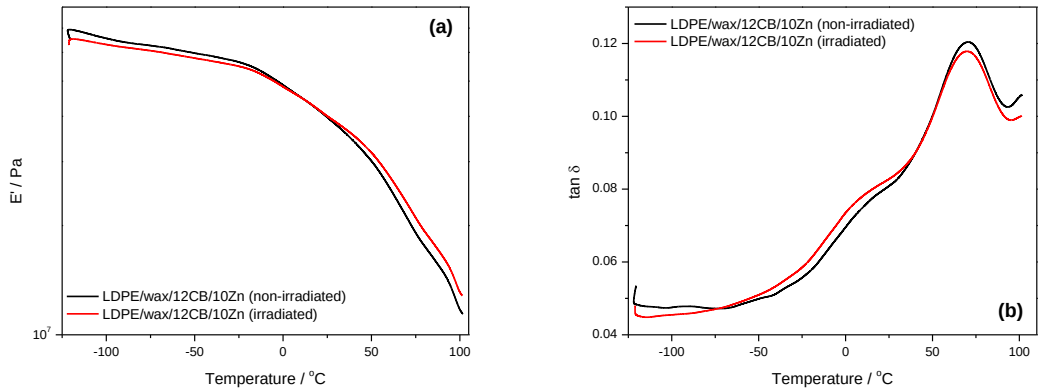

Figure 3.19 Effect of irradiation on the DMA results of LDPE/wax/12CB/10Zn composites

3.4 Electrical properties

3.4.1 Electrical conductivity

The thermo-electrical properties of a material refer to its change in electrical resistivity with temperature. Electrical switching can be attained by filling a semi-crystalline polymer with electrically conductive fillers. In this study, three different polyolefins have been used for this purpose, i.e. LDPE, HDPE and iPP. Due to structural differences between the three matrices and the temperature range of investigation for material application, which is from 20 to 95 °C, only the LDPE composites exhibited switching behaviour. However, in the same temperature range, the HDPE and iPP composites showed good electrical stability and can consequently be used for anti-static applications.

Figure 3.20 shows the room temperature resistivity results for the three polyolefins filled with 12 and 22 vol.% CB, and with 12 vol.% CB and 10 vol.% Zn. The effect of CB content, filler type, matrix type, and blending can be deduced from this picture. All the composites show significantly lower resistivity than the neat polymers, that have resistivity values ranging from 10^{14} to 10^{17} Ω cm, in line with literature [13]. The resistivity decreased with increasing CB content, which can be attributed to the increased number of conductive particles in the matrices that readily formed conductive networks. A resistivity drop of up to four orders of magnitude was observed as the CB loading was increased from 12 to 22 vol.%.

A decreasing trend in resistivity was observed in the order LDPE > HDPE > iPP for the composites filled with 12 vol.% CB. This can be largely ascribed to the differences in crystallinities of the polymers. iPP has a higher crystallinity than the polyethylenes, while HDPE is more crystalline than LDPE (section 3.2). Highly crystalline matrices comprise small amorphous fractions, which makes it easier for a conductive network to form, since filler particles preferentially reside in the amorphous domains of semi-crystalline polymers. The ordered crystal lamellae in crystalline regions reject these particles, while in polymers such as LDPE, since it is largely amorphous, a higher level of loading is required to attain the same conductivity. For the 22 vol.% CB content, although HDPE is more crystalline than LDPE, the two polyethylene composites behaved similarly, while the iPP composite still showed a higher conductivity. The melting enthalpy of HDPE decreased from 210 J g^{-1} for neat HDPE to 127 J g^{-1} for HDPE filled with 22 vol.% CB, while a decrease of only 30 J g^{-1} was observed for LDPE (Table 3.1). It is known that more crystalline matrices undergo electrical percolation at much lower filler contents than polymers with lower crystallinities [14], and it was also reported that the mobility of charge carriers (which is directly proportional to the resulting conductivity) in a crystalline polymer is significantly higher than in amorphous polymers [15]. Therefore, since high CB loadings obviously suppress the crystallization process, and since polymer crystals are more electrically conductive than amorphous chains, the observed relatively lower than expected conductivities in the HDPE composites can be attributed to this decrease in crystallinity.

Higher conductivities are observed with the additional incorporation of 10 vol.% Zn metal into the 12 vol.% CB composites, which can be attributed to the increased number of conductive particles. The 22 vol.% CB composites, however, show higher conductivities than the 12 vol.% plus 10 vol.% Zn composites, which is surprising since Zn has a much higher electrical conductivity than CB (volume resistivity of CB is approximately 10^{-3} [16] and that of Zn 10^{-6} Ω cm [13]). The reason for the lower conductivity in the presence of Zn could be poor interaction between the two, and possibly the nucleating ability of Zn particles. It will be easier for CB particles alone to form conductive pathways than for CB combined with Zn, since they have a higher affinity for each other than the affinity between CB and Zn. Furthermore, since the Zn particles are more effective nucleating centres for the crystallization of polyolefins (section 3.2), they are more likely to be covered with a polymer layer which will effectively separate them from neighbouring conductive particles.

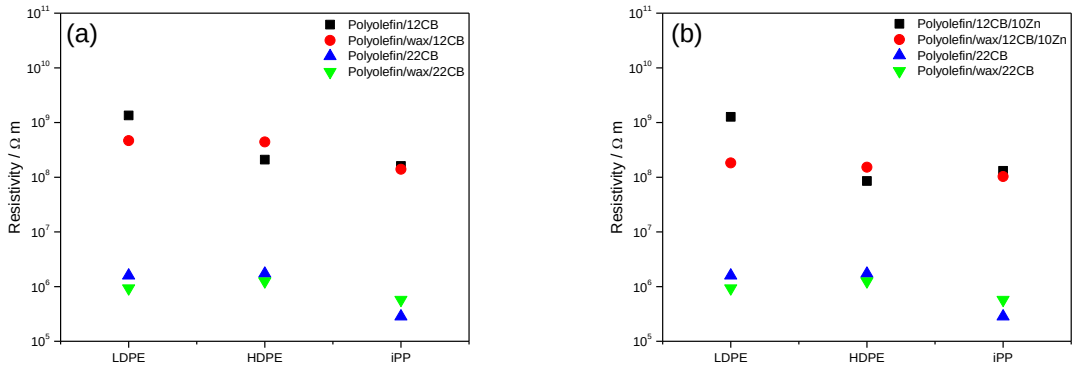

Figure 3.20 Room temperature resistivity of different polyolefin composites

The effect of blending with wax is more pronounced at low CB loadings, which is not surprising because highly conductive materials are less sensitive to structural changes. This corresponds well with our DMA observations (section 3.3), where it was observed that in a highly filled polymer matrix, wax had little influence on the storage modulus of the composites, since the stiffness was mostly determined by the amount of CB in the samples. Larger numbers of conductive particles give rise to more stable conductive networks, and therefore, any structural changes are less likely to affect these networks. Therefore, the presence of wax had less influence on the conductivities of the 22 vol.% CB containing composites. The presence of wax, irrespective of the filler loading, generally caused a slight increase in conductivity, which could be due to the higher crystallinities of the blend composites (section 3.2). Increased crystal lamellae reject the conductive particles and force them into the smaller amorphous portions, which thus increase the effective conductivity of the composites at the same filler loading. This effect is, however, less prominent in the highly-filled CB composites, since the bulk conductivity of the materials now depend on the amount of CB present in the composites, rather than on the slightly higher crystallinity. The irradiated samples generally showed higher resistivity values than the non-irradiated samples (Table 3.3), which can be ascribed to a disruption in the conductive pathways, decreased mobility of the polymer chains, and restricted agglomeration of CB and Zn particles due to intermolecular crosslinking.

Table 3.3 Resistivity of polyolefin-based composites before and after thermal ageing

Composites	Non-irradiated		Irradiated	
	Resistivity / Ω m (before ageing)	Resistivity / Ω m (after ageing)	Resistivity / Ω m (before ageing)	Resistivity / Ω m (after ageing)
LDPE/12CB	1.94E8	1.63E8	9.09E8	8.16E8
LDPE/wax/12CB	1.28E8	4.34E7	6.06E8	5.78E8
LDPE/22CB	5.19E5	4.28E5	1.13E6	8.37E5
LDPE/wax/22CB	2.78E5	2.27E5	6.26E5	4.67E5
HDPE/12CB	8.83E7	7.35E7	1.82E8	1.55E8
HDPE/wax/12CB	1.79E8	1.27E8	1.91E8	1.38E8
HDPE/22CB	9.43E5	7.69E5	9.76E5	7.77E5
HDPE/wax/22CB	3.40E5	3.09E5	9.06E5	6.69E5
iPP/12CB	1.08E8	9.04E7	1.60E5	1.33E5
iPP/wax/12CB	4.26E7	4.10E7	2.83E5	2.17E5
iPP/22CB	1.68E5	1.47E5	1.56E3	1.32E3
iPP/wax/22CB	1.90E5	1.53E5	9.99E3	6.13E3

3.4.2 Thermo-switching

Polyolefins are a group of polymers that can be crosslinked by irradiation. The effective gamma irradiation dose that produces a network can range up to 300 kGy. In this study, the samples were irradiated using 100 kGy at room temperature. At low irradiation dose, the extent of crosslinking, which preferentially occurs in the amorphous parts of the polyolefins, determines the properties of the materials. However, at very high irradiation doses, degradation effects such as chain scission and oxidation are dominant. In this study, all the composites showed semi-conductive behaviour at ambient temperature, exhibiting a decrease in resistivity with an increase in temperature, in contrast to highly conductive metals, which behave in the opposite manner. However, these materials still show semi-conductive transitions at higher temperatures, with the HDPE and iPP composites having good electrical stability while the LDPE composites have a strong resistivity-temperature dependence in the investigated temperature range.

3.4.2.1 LDPE/CB composites

Figure 3.21 shows the electrical thermo-switching curves of the LDPE/CB and LDPE/12CB/10Zn composites. The 12 vol.% CB composites display switching at ~ 85-90 °C, but the switching temperature shifted to higher temperatures for the 22 vol.% CB composites. It was shown in section 3.3 that the higher filler content caused a reduction in the intensity of the α-relaxation, suggesting decreased mobility of the polymer chains in the crystalline regions, which was a consequence of their immobilisation by the filler particles. More energy will therefore be needed to deform the conductive pathways, and hence the switching shifted to higher temperatures. The switching temperature did not change in the case of the 12CB/10Zn hybrid composites. Since CB was shown to have a much stronger interaction with LDPE than Zn, the immobilization effect on the matrix chains by the filler particles in the Zn-containing samples was less pronounced, and less energy was required for breaking up the conductive network, hence the switching occurred at a lower temperature. The presence of wax did not have a significant influence on the switching temperature. This can be ascribed to the single melting temperature for these samples because of the co-crystallization of the wax with LDPE.

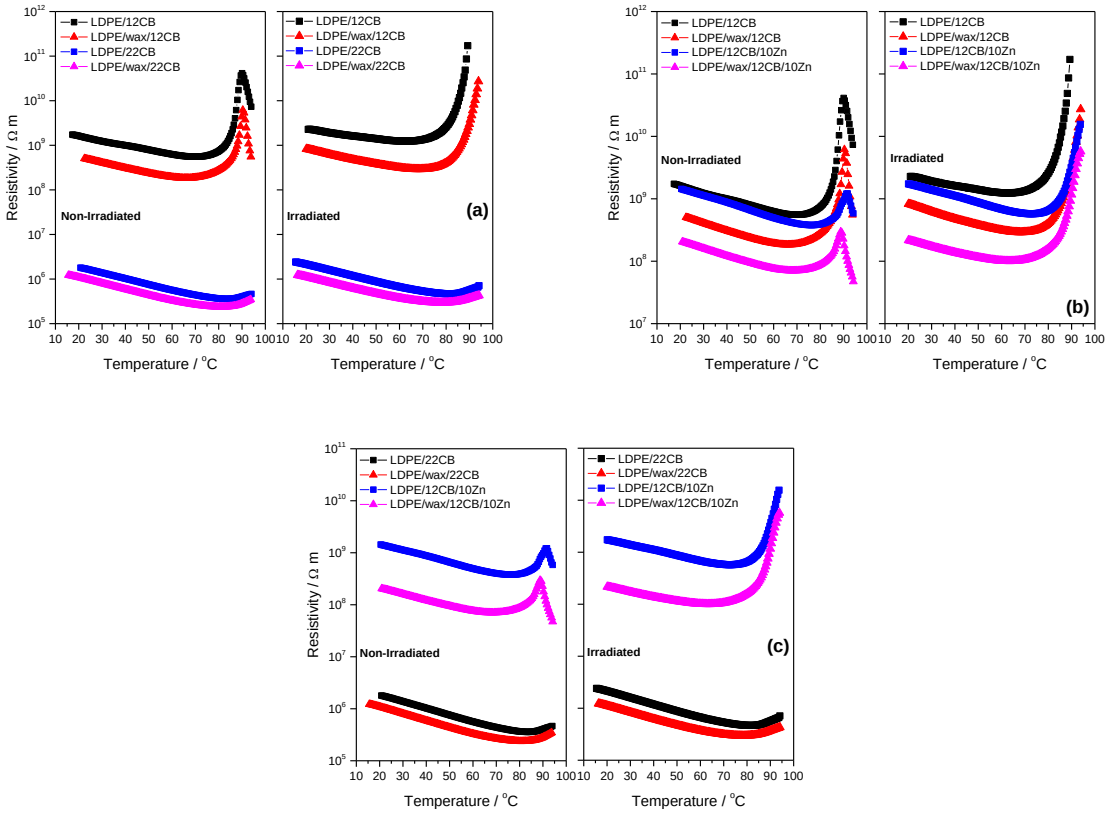

Figure 3.21 Switching curves of irradiated and non-irradiated LDPE composites

The PTC intensity of the composites decreased significantly with the addition of Zn particles (Figure 3.21). The density of Zn is significantly higher than that of CB, and therefore more energy is needed to separate them and completely break up the conductive pathways. Moreover, due to the weak interaction between the two fillers, it is possible that there are two independent conductive networks within the composites: one consisting of CB particles and the other being made up of Zn particles. This would mean that the CB particles will detach independently of the Zn particles. Although the PTC effect will occur when the CB network breaks, it is possible that at the same temperature, part of the Zn network will remain intact, which would sustain the levels of conductivity, and hence the low increase in resistivity compared to the 12 vol.% CB composites. Wax did not significantly influence the PTC intensity in the low CB content composites, but it caused a slight increase in PTC intensity in the Zn-containing samples. The Zn particles were shown to increase the crystallinity of the hybrid composites, and the larger thermal expansion of the more crystalline matrices probably caused this increase. In one study, the influence of crystalline and aggregate structures on the PTC characteristics and resistivity behaviour of HDPE/CB, LDPE/CB, EVA/LDPE/CB and PMMA/CB was compared [17]. All the composites exhibited the PTC effect, but the PTC intensity of the PMMA/CB system was very low, since it had the lowest crystallinity. The HDPE/CB composites showed the highest PTC intensity due to the larger expansion accompanying crystalline melting.

The irradiated samples generally showed an increased PTC intensity (Figure 3.21), which can be ascribed to the presence of a crosslink network in the composites. In a crosslinked sample, the expansion of the matrix is restricted. This means that when the conductive network breaks and the conductive particles detach from each other, their movement is restricted, which increases the bulk resistivity of the composites. It also becomes less likely that the particles will re-agglomerate and form conductive paths at elevated temperatures, since they will be enclosed in the crosslinked network which will restrict their migration. This behaviour was also observed in other investigations. For example, in one study, where the influence of electron beam irradiation on the PTC/NTC behaviour of HDPE/carbon black conducting polymer composites was investigated [18], the movement of the CB particles was reduced significantly, since intermolecular crosslinking markedly reduced the mobility of the segments. The agglomeration of the CB particles was therefore restricted and a higher PTC intensity was observed for the irradiated samples.

All the composites showed a mild NTC effect at lower temperatures, due to the thermal activation of electrons. As the temperature increases, the electrons gain energy and become charge carriers, which facilitates conduction and increases the effective conductivity of the materials. Although we did not present curves at higher temperatures, we selected the LDPE/12CB and LDPE/12CB/10Zn composites to show the influence of irradiation on the NTC effect (Figure 3.22), since they exhibited switching behaviour. It can be clearly seen that irradiation was effective in reducing the NTC intensity, and thus eliminating the NTC effect. This can be ascribed to the presence of a crosslink network in the LDPE matrix, which reduced the mobility of the intermolecular segments, preventing the unwanted re-agglomeration of CB particles at elevated temperatures. The wax-containing irradiated samples also showed a significantly reduced NTC intensity, which suggests that the highly crystalline wax did not have an adverse effect on the stability imparted by irradiation on the composites, which is advantageous since electrical stability is crucial in thermo-electrical applications.

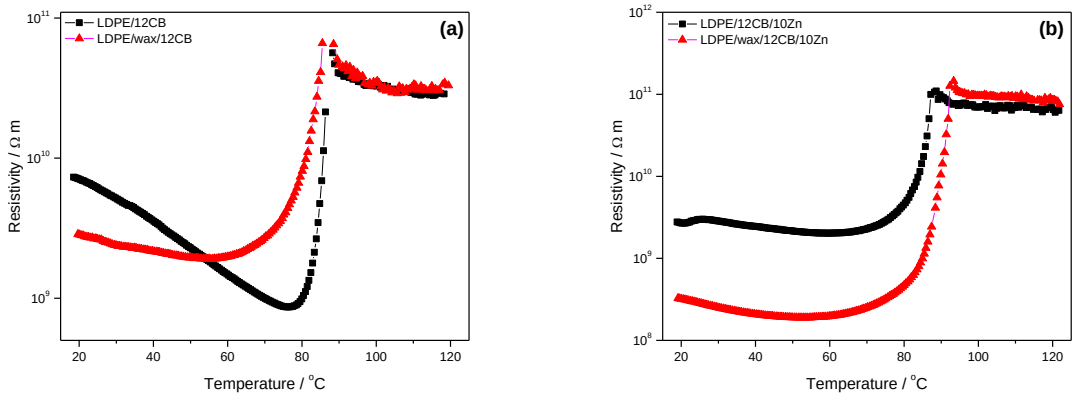

Figure 3.22 Switching curves of irradiated (a) LDPE/12CB and (b) LDPE/12CB/10Zn composites

3.4.2.2 HDPE/CB composites

The resistivity behaviour of the HDPE/CB and HDPE/12CB/10Zn hybrid composites is illustrated in Figure 3.23. Similar behaviour to that of the LDPE composites was observed, with all the composites showing low resistivities compared to that of the pure polymer, and with the resistivities decreasing with increasing CB content. The resistivities in all the composites continuously decreased with increasing temperature, which can be ascribed to the thermal activation of the electrons. Wax had little effect on the conductivity levels, and its

influence was uniform throughout the temperature range of analysis. The higher values for the wax-containing samples are probably because wax increased the crystallinity of the composites, which was accompanied by a corresponding increase in conductivity, as discussed earlier. None of the HDPE-based composites showed any switching behaviour, and wax also did not induce switching around its melting temperature. This is probably due to the co-crystallization of wax with the matrix polymer and the melting of all the crystals in the same temperature range. The irradiated and non-irradiated, neat and blended composites showed a fairly stable resistivity behaviour in the temperature range of investigation, and the resistivity decrease with increasing temperature was less than an order of magnitude. This makes these cheap materials suitable for the dissipation of static charge, and they are therefore good candidates for anti-static applications, where the stability of electrical resistivity with temperature is a requirement.

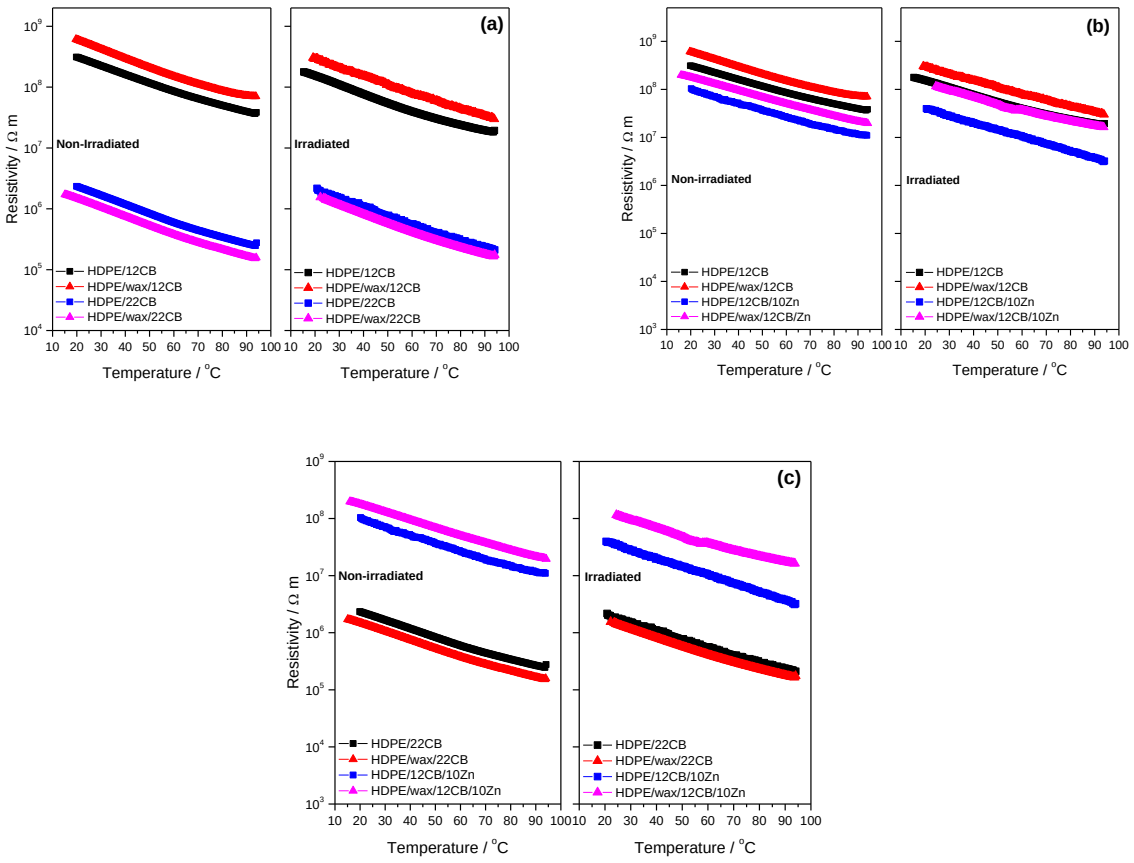

Figure 3.23 Switching curves of irradiated and non-irradiated HDPE-based composites

3.4.2.3 iPP/CB composites

Figure 3.24 shows the resistivity behaviour of the iPP/CB and iPP/12CB/10Zn composites. The general behaviour was similar to that of the HDPE composites.

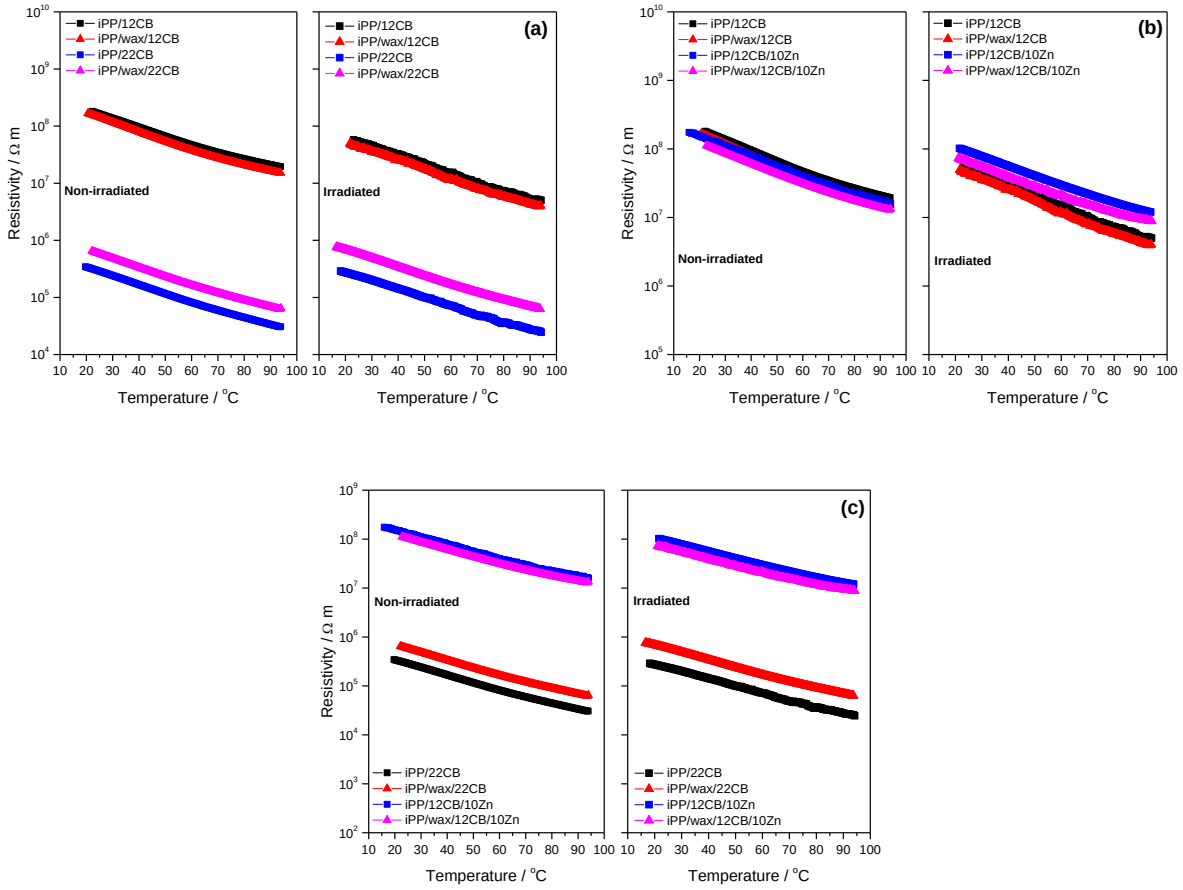

Figure 3.24 Switching curves of irradiated and non-irradiated iPP-based composites

3.4.3 Thermo-electrical stability

Thermo-electrical stability refers to the reproducibility of the resistivity behaviour with temperature during thermal cycling. Since these composites are to be used for thermo-sensing applications, the samples were subjected to three heating and cooling cycles, using 2 and 3 °C min^{-1} heating and cooling rates, between 20 and 70 °C, and during this process the resistivity behaviour was monitored. The results are shown in Figures 3.25 and 3.26. The upper limit of the temperature range was chosen to correlate with the temperature range for practical material application. The resistivity decreased during heating, meaning that the composites became more conductive with increasing temperature, which was probably due to the high

thermal energy available for electrons to facilitate conduction. It can be seen that all the composites, irradiated and non-irradiated, exhibit good electrical stability during thermal cycling, as was evident from the reproducible resistivity behaviour in the temperature range of analysis.

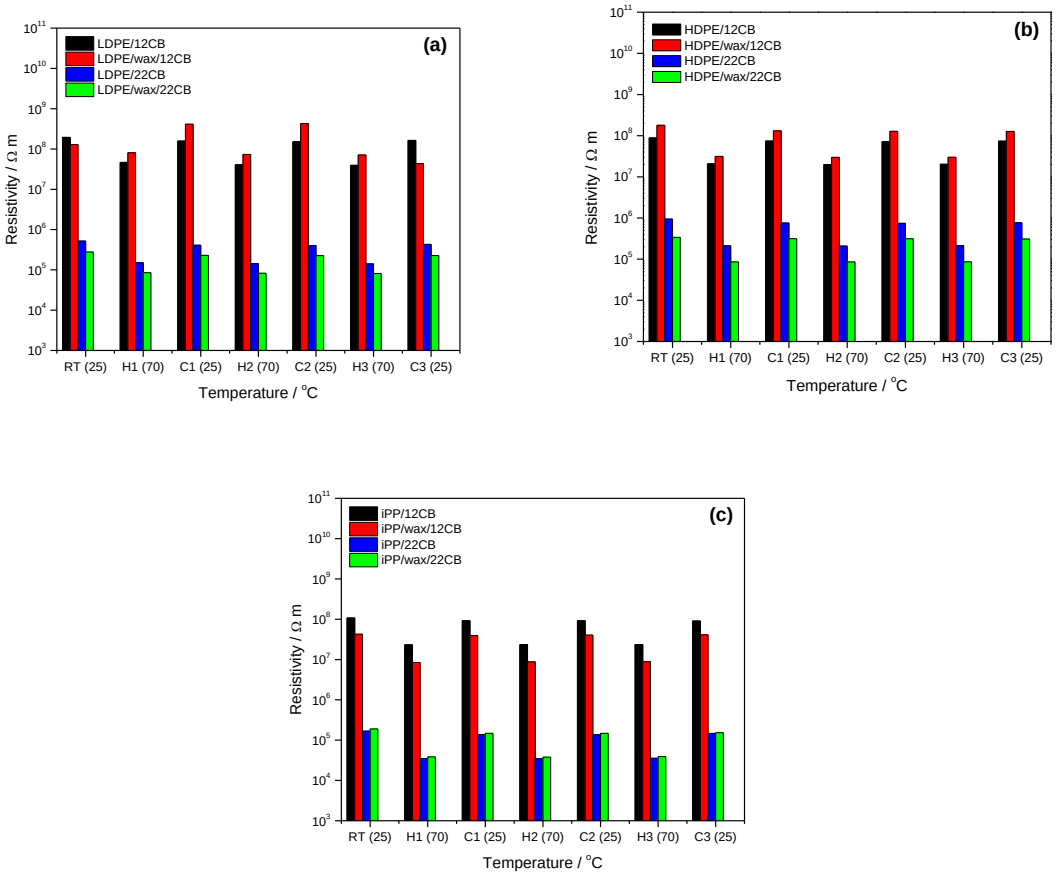

Figure 3.25 Thermal cycling results of non-irradiated (a) LDPE/CB, (b) HDPE/CB and (c) iPP/CB composites (RT – room temperature; H – heating; C – cooling)

Table 3.3 shows the resistivity values at room temperature before and after thermal ageing. The percentage change in resistivity after thermal ageing, as well as the maximum change in resistivity at 70 °C during thermal cycling, are reported in Figures 3.27 and 3.28 for the LDPE, HDPE and iPP composites. The values were calculated using Equations 3.3 and 3.4.

$$\text{Change in resistivity after thermal ageing} = \frac{Ra-Rrt}{Rrt} \times 100\% \qquad (3.3)$$

$$\text{Maximum change in resistivity at 70 °C} = \frac{R70-Rrt}{Rrt} \times 100\% \qquad (3.4)$$

where R_{rt}, R_a and R_{70} represent the resistivities at room temperature, after ageing, and at 70 °C, respectively.

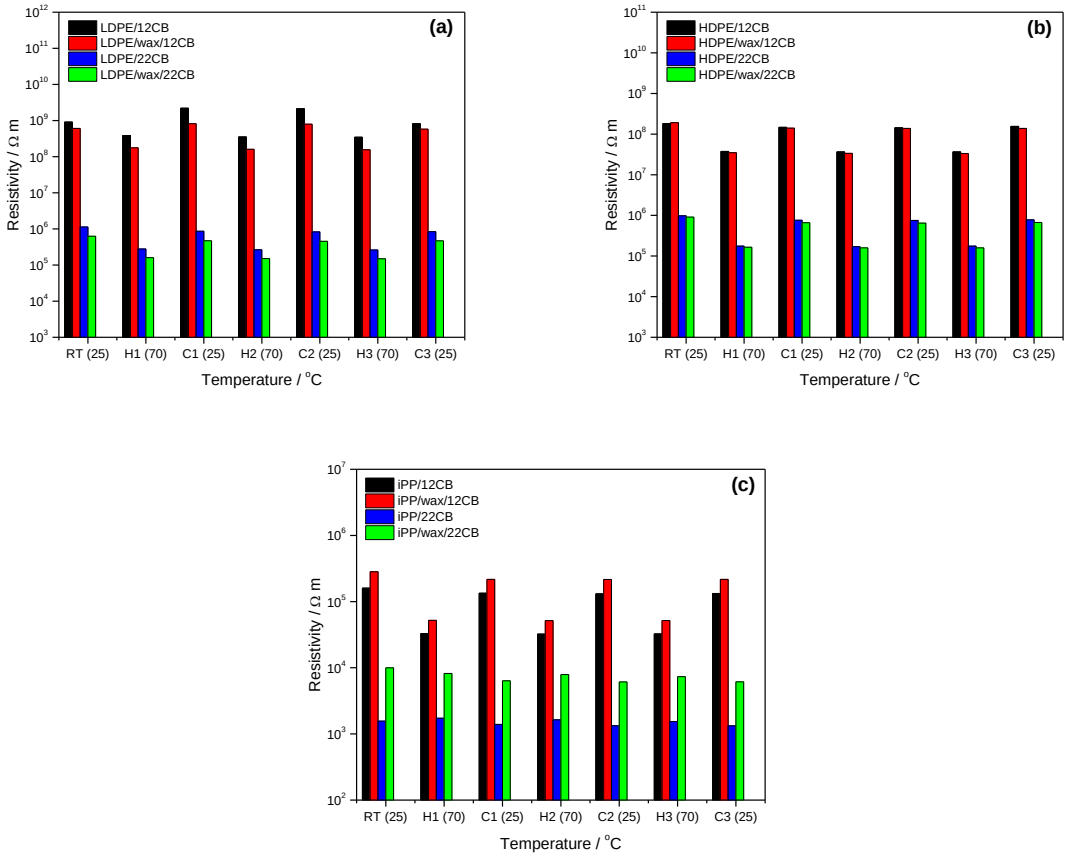

Figure 3.26 Thermal cycling results of irradiated (a) LDPE/CB, (b) HDPE/CB and (c) iPP/CB composites (RT – room temperature; H – heating; C – cooling)

All the samples show a drop in resistivity due to thermal ageing, which could be attributed to increased crystallinity in the samples as a result of the recrystallization of smaller polyolefin crystals. It has been reported in literature [19,20] that when polyethylene and polypropylene undergo thermal ageing, reorganization of the crystalline phase occurs, which leads to an increase in its perfection due to relief of local stresses in the strained regions of the crystals. Therefore, the reduction in resistivity brought about by an increase in crystallinity can be attributed to an increase in lamellar perfection and/or thickening. This effect is more pronounced in most of the wax-containing samples, and could be the result of shorter wax chains being incorporated into the crystal structure during secondary crystallization. However, most of the irradiated samples show only a small decrease in resistivity after ageing, which is

probably because of the presence of a crosslink network induced by γ-irradiation. It is known that crosslinking can result in more stable conductive behaviour in thermo-switch materials [18]. The relatively good electrical stability of these materials, even after being subjected to thermal cycling, shows that there are no significant structural changes in the materials during thermo-sensing applications, and hence the resistivity changed only little after thermal ageing. Such a small resistivity decrease with temperature is beneficial, since a big decrease would lead to high conductivity, which is practically dangerous. Relatively low levels of conductivity are good, especially in anti-electrostatic applications. Anti-static materials have very good static dissipative qualities since they can effectively prevent the build-up of static charge. However, high conductivity due to an increase in temperature can render the materials conductive, which can lead to electric shock when these materials are used to protect people from the flowing current within electronic devices.

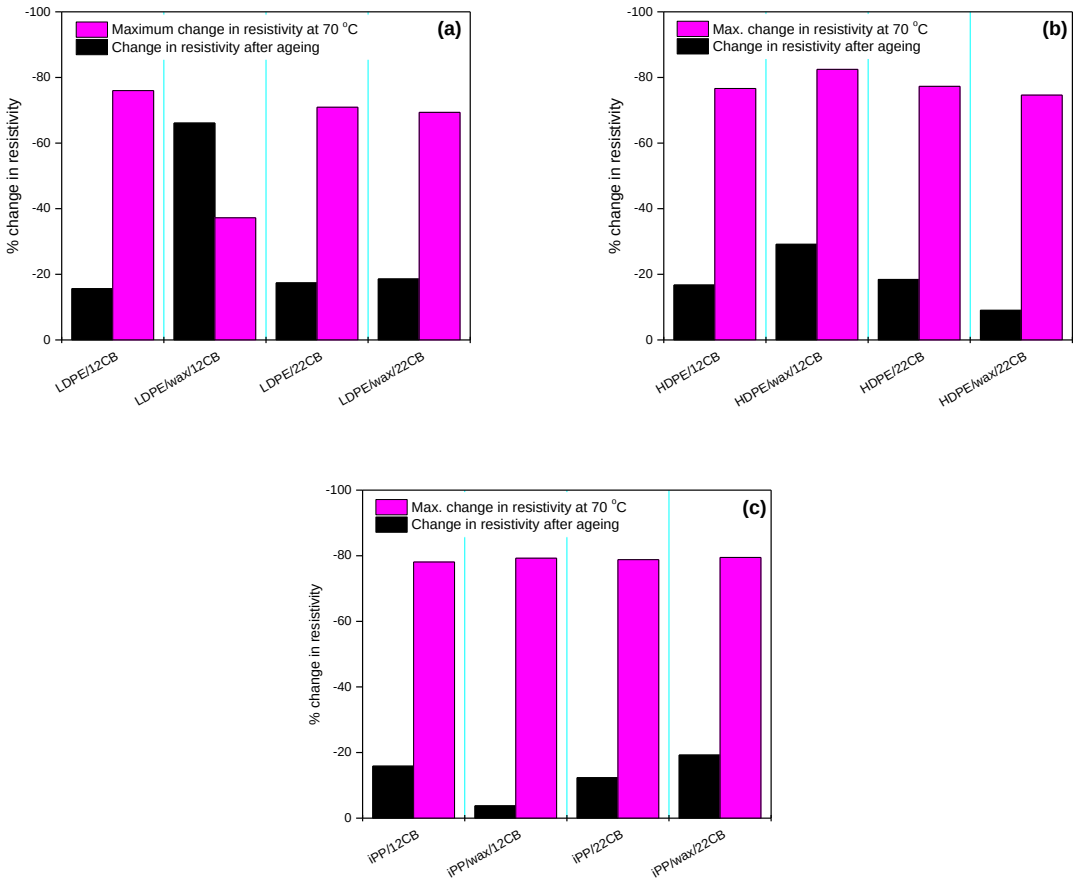

Figure 3.27 Percentage change in resistivity of non-irradiated (a) LDPE/CB, (b) HDPE/CB and (c) iPP/CB composites

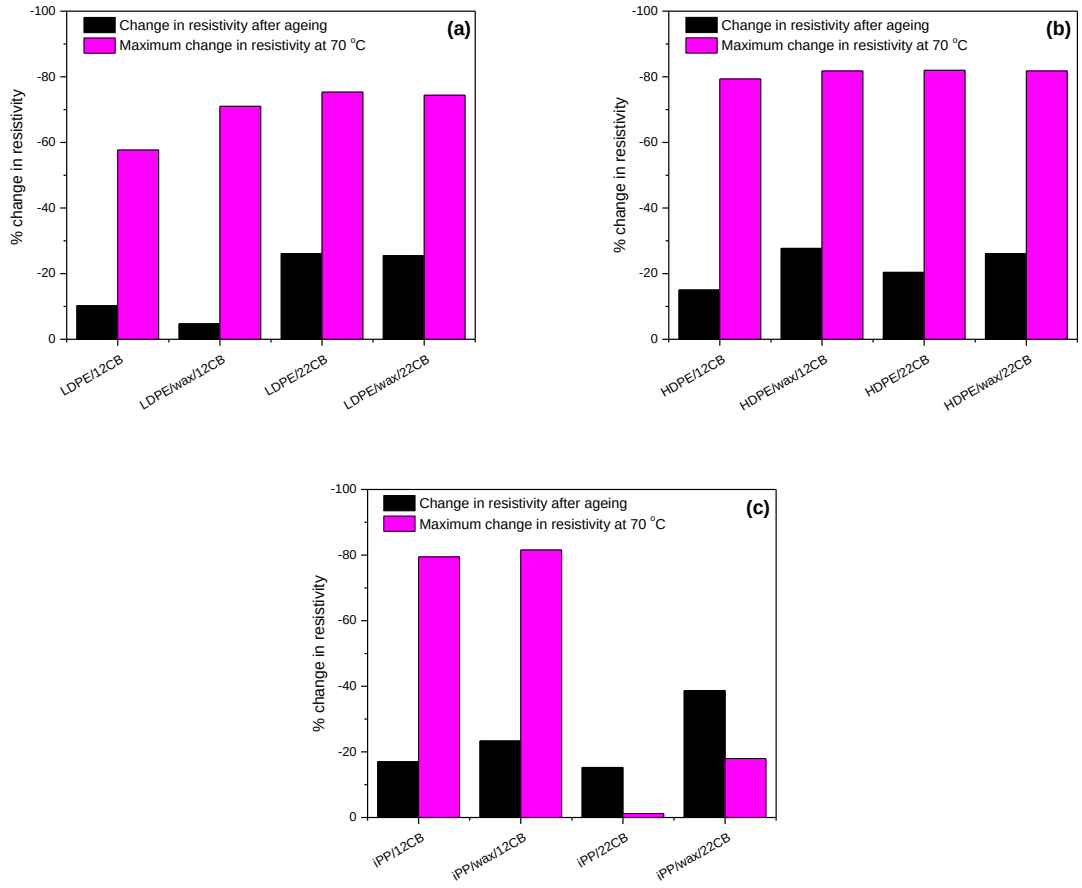

Figure 3.28 Percentage change in resistivity of irradiated (a) LDPE/CB, (b) HDPE/CB and (c) iPP/CB composites

3.5 Impact testing

Polymeric materials, especially semi-crystalline polymers, possess good mechanical properties such as ductility and strength at ambient temperature or under low to moderate levels of stress [21]. The incorporation of fillers into polymer matrices generally gives rise to cost-effective materials with improved physical properties. However, there are some undesirable effects as well, which include the deterioration of impact properties [22]. The mechanical properties of composite materials are determined by the volume fraction of the fillers, their physical form and the interfacial adhesion between the filler particles and the matrix [23]. In this study, HDPE was one of the polymers blended with wax and filled with different CB contents, as well as with a hybrid 12CB/10Zn filler.

Figure 3.29 presents the impact properties of neat HDPE, as well as its blends and composites. Blending of HDPE with wax clearly results in a significant reduction in the impact strength. This can be attributed to the poor impact properties of the highly crystalline wax, and to the wax crystals that formed defect centres inside the polymer matrix. It is known that brittle materials or particles cannot effectively stop or stabilize crack propagation [24].

A decrease in impact strength was observed for the different composites prepared in the absence of wax, irrespective of the filler type or loading. Various factors can play a role in fillers reducing the impact properties of a polymer, like the elasticity of the composites, particle size, filler aspect ratio, rigidity, concentration, the matrix-filler interaction and nucleation. However, rigid micro-sized filler particles normally reduce the impact strength because they act as stress concentrators for the development of cracks.

The presence of wax further deteriorated the impact properties of the different composites, except in the case of HDPE/wax/12CB (Figure 3.29). This could be the result of the wax, having a weaker interaction with the matrix than the filler, covering the filler particles. The wax could also have formed separate crystals in the HDPE matrix, which would increase the number of defect centres in these composites.

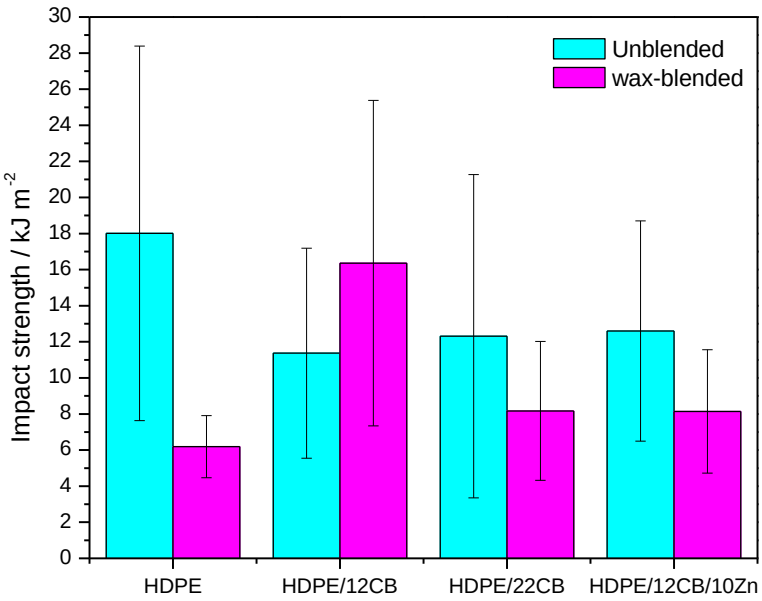

Figure 3.29 Impact strengths of pure HDPE and its respective blends and composites

It is, however, difficult to explain the impact strength of the HDPE/wax/12CB composite. We therefore took a closer look at our Charpy impact data. As can be seen in Table 3.4, the impact tests on eight samples gave four fairly low values, and four much higher values. Since we ran out of samples and could not do any further tests, and since we had no grounds to decide on using only certain of these values, we took the average of all these values which gave a value that is out of line with the rest of the results.

Table 3.4 Impact strengths of eight samples from the HDPE/wax/12CB composite

Impact strength / kJ m^{-2}	
4.49	22.32
8.46	22.53
9.09	23.43
11.33	29.19

3.6 References

[1] J.A. Molefi, A.S. Luyt, I. Krupa, Investigation of thermally conducting phase change materials based on polyethylene/wax blends filled with copper particles. Journal of Applied Polymer Science 2010; 116:1766-1774.
DOI: 10.10022/app.31653

[2] I. Krupa, I. Novák, I. Chodák. Electrically and thermally conductive polyethylene/ graphite composites and their mechanical properties. Synthetic Metals 2004; 145:245-252.
DOI: 10.1016/j.synthmet.2004.05.007

[3] I. Novák, I. Krupa, I. Janigová. Hybrid electro-conductive composites with improved toughness filled by carbon black. Carbon 2005; 43:841-848.
DOI: 10.1016/j.carbon.2004.11.019

[4] Q.-H. Zhang, D.-J. Chen. Percolation threshold and morphology of composites of conducting carbon black/polypropylene/EVA. Journal of Materials Science 2004; 39:1751-1757.
DOI: 10.1023/B:JMSC.0000016180.42896.0f

[5] M.P. Molaba, D. Dudić, A.S. Luyt. Influence of the presence of medium-soft paraffin wax on the morphology and properties of iPP/silver nanocomposites. eXPRESS Polymer Letters 2015; 10:901-915.
DOI: 10.3144/expresspolymlett.2015.82

[6] S.P. Hlangothi, I. Krupa, V. Djoković, A.S. Luyt. Thermal and mechanical properties of cross-linked and uncross-linked linear low-density polyethylene-wax blends. Polymer Degradation and Stability 2003; 79:53-59.
PII: S0141-3910(02)00238-0

[7] I. Krupa, A.S. Luyt. Thermal properties of uncross-linked and cross-linked LLDPE/wax blends. Polymer Degradation and Stability 2000; 70:111-117.
DOI: 10.1016/S0141-3910(00)00097-5

[8] T.N. Mtshali, I. Krupa, A.S. Luyt. The effect of cross-linking on the thermal properties of LDPE/wax blends. Thermochimica Acta 2001; 380:47-54.
DOI: 10.1016/S0040-6031(01)00636-0

[9] R.O. Sirotkin, N.W. Brooks. The dynamic mechanical relaxation behaviour of polyethylene copolymers cast from solution. Polymer 2001; 42:9801-9808.
DOI: 10.106/S0032-3861(01)00535-3

[10] M.A. Milani, D. González, R. Quijada, N.R.S. Basso, M.L. Cerrada, D.S. Azambuja, G.B. Galland. Polypropylene/graphenenanosheet nanocomposites by *in situ* polymerization: Synthesis, characterization and fundamental properties. Composites Science and Technology 2013; 84:1-7.
DOI: 10.1016/j.compositech.2013.05.001

[11] K.P. Menard. Dynamic Mechanical Analysis: A Practical Introduction. CRC Press: Boca Raton, USA 1999; 100-123.

[12] S.P. Hlangothi, I. Krupa, V. Djoković, A.S. Luyt. Thermal and mechanical properties of cross-linked and uncross-linked linear low-density polyethylene–wax blends. Polymer Degradation and Stability 2003; 79:53-59.
PII: S0141-3910(02)00238-0

[13] H.S. Katz, J.V. Milewski. Handbook of Fillers for Plastics. Van Nostrand Reinhold, New York (1987).
ISBN: 0-442-26024-5

[14] J.-C. Huang. Review: Carbon black filled conducting polymers and polymer blends. Advances in Polymer Technology 2002; 21:299-313.

[15] V.E. Gul'. Structure and Properties of Conducting Polymer Composites (New Concepts in Polymer Science). CRC Press, Utrecht (1996).

ISBN: 978-9067642040

[16] D.C. Giancoli. Physics: Principles with Applications 4th Ed. Prentice Hall, New Jersey (1995).
ISBN: 978-0131021532

[17] Y. Luo, G. Wang, B. Zhang, Z. Zhang. The influence of crystalline and aggregate structure on PTC characteristic of conductive polyethylene/carbon black composite. European Polymer Journal 1998; 34:1221-1227.
PII: S0014-3057(98)00099-8

[18] M.-K. Seo, K.-Y. Rhee, S.-J. Park. Influence of electro-beam irradiation on PTC/NTC behaviours of carbon blacks/HDPE conducting polymer composites. Current Applied Physics 2011; 11:428-433.
DOI: 10.1016/j.cap.2010.08.013

[19] D. Dudić, D. Kostoski, V. Djoković, Z. Stojanović. Recrystallization processes induced by accelerated ageing in isotactic polypropylene of different morphologies. Polymer Degradation and Stability 2000; 67:233-237.
DOI: 10.1016/S0141-3910(99)00118-4

[20] S.K. Bhateja, E.H. Andrews, S.M. Yarbrough. Radiation induced crystallinity changes in linear polyethylenes: Long term aging effects. Polymer Journal 1989; 21:739-750.
DOI:10.1295/polymj.21.739

[21] D. Eiras, L.A. Pessan. Mechanical properties of polypropylene/calcium carbonate nanocomposites. Materials Research 2009; 4:517-522.
DOI: 10.1590/S1516-14392009000400023

[22] I. Švab, V. Musil, I. Šmit, M. Makarovič. Mechanical properties of wollastonite-reinforced polypropylene composites modified with SEBS and SEBS-g-MA elastomers. Polymer Engineering and Science 2007; 47:1873-1880.
DOI: 10.1002/pen.20897

[23] M. Taşdemir, H.Ö. Gülsoy. Mechanical properties of polymers filled with iron powder. International Journal of Polymeric Materials and Polymeric Biomaterials 2008; 57:258–265.
DOI: 10.1080/00914030701473656

[24] A. Lazzeri, S.M. Zebarjad, M. Pracella, K. Cavalier, R. Rosa. Filler toughening of plastics. Part 1 - The effect of surface interactions on physico-mechanical properties and rheological behaviour of ultrafine $CaCO_3$/HDPE nanocomposites. Polymer 2004; 46:827-844.
DOI: 10.1016/j.polymer.2004.11.111

CHAPTER FOUR

CONCLUSIONS

The main purpose of this project was to investigate the effect of CB content, medium-soft Fischer-Tropsch paraffin wax, γ-irradiation and Zn metal powder as second filler on the thermal and mechanical properties, and thermo-electrical behaviour of polyolefin/CB composites, and the objectives stated in Chapter 1 were reached to a large extent.

Differences between the dispersions of CB, and CB and Zn in the hybrid composites, suggest that there was a fairly weak interaction between the two fillers which would have influenced the successful formation of conductive pathways in the composites that contained both CB and Zn. The crystallinity decreased with an increase in CB loading in all the investigated samples, and this was attributed to the immobilization of the polymer chains through interaction with the CB particles. The presence of Zn, however, gave rise to higher crystallinities, which was ascribed to the Zn particles acting as effective nucleation centres for the crystallization of the polyolefins. There was a fairly strong general increase in crystallinity with the addition of wax, which was attributed to the co-crystallization of the shorter wax chains with the polymer chains. The irradiated samples showed lower crystallinities than the non-irradiated samples, which was ascribed to the presence of crosslinks, which immobilized the polymer chains and suppressed crystallization.

The storage modulus values of the composites were significantly higher than those of neat LDPE throughout the investigated temperature range, and this was attributed to the presence of rigid CB and Zn particles that imparted stiffness to the samples. However, the storage modulus decreased when wax was present, and this was ascribed to the softness of the wax compared to that of LDPE. The presence of the filler particles significantly decreased the intensity of the α-transition because of the decreased crystallinity of the LDPE and the immobilisation of the polymer chains by the filler particles in the inter-crystalline amorphous regions. The presence of wax, however, caused the α-relaxation to shift to slightly higher temperatures and increased its intensity. This was the result of the wax melting in the same temperature range as the α-transition. Blending of HDPE with wax resulted in a significant reduction in the impact strength because of the poor impact properties of the highly crystalline wax, and because of the wax crystals forming defect centres inside the polymer matrix. The impact strength was also lower for the filler-containing samples, because the rigid filler

particles acted as stress concentrators for the development of cracks. The wax and filler particles were found to have an additive effect on the reduction of the impact properties.

Electrical switching can be attained by filling a semi-crystalline polymer with electrically conductive fillers. In this study, three different polyolefins were used for this purpose. All the composites showed semi-conductive behaviour at ambient temperature, exhibiting a decrease in resistivity with an increase in temperature due to the thermal activation of electrons. A decreasing trend in resistivity was observed in the order LDPE > HDPE > iPP for the composites filled with lower CB content. This was largely ascribed to the differences in crystallinity of the polymers. iPP had the highest degree of crystallinity while LDPE had the lowest. Due to structural differences between the three matrices and the temperature range of investigation for material application, which was from 20 to 95 °C, only the LDPE composites exhibited switching behaviour. However, in the same temperature range, the HDPE and iPP composites showed good electrical stability and can consequently be used for anti-static applications.

All the composites showed significantly lower resistivity than the neat polymers, and the resistivity decreased with increasing CB content, which was attributed to the increased number of conductive particles in the matrices that readily formed conductive networks. Increased conductivities were also observed with the additional incorporation of 10 vol.% Zn metal into the 12 vol.% CB composites, which was also attributed to the increased number of conductive particles. The 22 vol.% CB composites, however, showed higher conductivities than the 12 vol.% plus 10 vol.% Zn composites. The reason for the lower conductivity in the presence of Zn could be the poor interaction between the two fillers, and possibly the nucleating ability of the Zn particles. The presence of wax, irrespective of the filler loading, generally caused a slight increase in conductivity, which was ascribed to the higher crystallinities of the blend composites. This effect, however, was more pronounced at low CB loadings. The irradiated samples generally showed higher resistivity values than the non-irradiated samples, which was ascribed to a disruption in the conductive pathways, decreased mobility of the polymer chains, and restricted agglomeration of CB and Zn particles due to intermolecular crosslinking.

The 12 vol.% CB composites displayed switching at ~ 85-90 °C, but the switching temperature shifted to higher temperatures for the 22 vol.% CB composites. This was

attributed to decreased mobility of the polymer chains in the crystalline regions, which was a consequence of their immobilisation by the CB particles. The switching temperature did not change in the case of the 12CB/10Zn hybrid composites. CB was shown to have a much stronger interaction with LDPE than Zn, and therefore the immobilization effect on the matrix chains by the filler particles in the Zn-containing samples was less pronounced. The presence of wax did not have a significant influence on the switching temperature. This was ascribed to the single melting temperature for these samples because of the co-crystallization of the wax with LDPE.

The PTC intensity of the 12 vol.% CB composites decreased significantly with the addition of Zn particles. This was ascribed to the high density of Zn compared to CB, and also to the weak interaction between the two fillers. Wax did not significantly influence the PTC intensity in the low CB content composites, but it caused a slight increase in PTC intensity in the Zn-containing samples. The Zn particles were shown to increase the crystallinity of the hybrid composites. The larger thermal expansion of the more crystalline matrices probably caused this increase. The irradiated samples generally showed a significantly increased PTC intensity, which was ascribed to the presence of a crosslink network in the composites.

All the composites showed a mild NTC effect at lower temperatures, due to the thermal activation of electrons. γ-irradiation was effective in reducing the NTC intensity, and thus eliminating the NTC effect. This was ascribed to the presence of a crosslink network in the LDPE matrix, which reduced the mobility of the intermolecular segments, preventing the unwanted re-agglomeration of CB particles at elevated temperatures. The wax-containing irradiated samples also showed a significantly reduced NTC intensity, which suggested that the highly crystalline wax did not have an adverse effect on the stability imparted by irradiation on the composites.

All the composites showed a drop in resistivity due to thermal ageing, which was attributed to increased crystallinity in the samples as a result of recrystallization effects. This effect was more pronounced in most of the wax-containing samples, and could be the result of shorter wax chains being incorporated into the crystal structure during secondary crystallization. However, most of the irradiated samples showed only a small decrease in resistivity after ageing compared to non-irradiated samples, which was probably because of the presence of a

crosslink network induced by γ-irradiation, which gave rise to more stable conductive behaviour in the materials.

Based on our findings, we identified some areas that still need further investigation. These include (i) the PTC mechanism in a thermo-switch system of two compatible fillers, (ii) the effect of the selective distribution of the filler particles on the PTC intensity, (iii) the effect of the nucleating ability of the filler particles on the formation of conductive networks and the resulting conductivity, (iv) the effect of irradiation dose on the thermo-mechanical properties of the composites, and (v), the effect of wax content on the room temperature resistivity, switching temperature and PTC intensity of the materials.

ACKNOWLEDGEMENTS

The carrying out of the study and the preparation of this thesis would not have been possible without the will of **Le Tout-Puissant Dieu** (The Almighty God, The One Who gave life, The Most High), and the support, hard work and endless efforts of my superiors and loved ones.

I would like to thank my supervisor, **Prof. Adriaan Stephanus Luyt,** for his great efforts in explaining things with clarity and simplicity. I express my deep sense of gratitude for his guidance, source of inspiration and constant support throughout the course of the study. During my thesis-writing period, he provided encouragement, sound advice, good teaching, good company, and lots of good ideas. His overly enthusiasm and integral view on research and his mission for providing only high-quality work has made a deep impression on me. I owe him lots of gratitude for introducing me to polymer science and the research world.
Baie dankie Prof!

I would like to gratefully acknowledge my enthusiastic and ambitious co-supervisor, **Dr. Duško Dudić.** Throughout this project, he shared with me a lot of his expertise and research insights. Although he was away from home (Belgrade, Serbia) for lengthy periods of time, it did not have an adverse effect on his level of performance and professionalism.
Много вам хвала Doctor!

I acknowledge the University of the Free State (UFS) at large by providing me with an opportunity to study, the National Research Foundation (NRF) (through Dr J.P. Mofokeng's Thuthuka grant) for financial support, and the Faculty secretary, Mrs Marlize Jackson, for her selfless service rendered.

I also wish to thank greatly my friends Mainangoana Gregory Motsoeneng, Pule Ntlatseng, Rethabile Rejoice Dlamini, Sabelo Sydney Makhanya, Lelesa Ezaya Tshabangu and The King Himself, **Él Deeré Bendiciòn de Souza Beninho** for helping me get through the tough times, true friendship and for all the good ideas shared.

Special thanks to my beloved family: I thank my parents Reuben and Maditaba for raising me with love, guidance and responsibility. I also wish to thank my only sibling (sister), Palesa, for her friendship, support and encouragement. If it was not for you guys, I would not have been The Man I am today, and for that, I owe you eternal gratitude…Merci beaucoup à tous!!!

Je suis De Souza, le chef de l'empire Deeré!